Supplemental information

Autophagy-regulating TP53INP2 mediates muscle wasting and is repressed in diabetes

David Sala, Saška Ivanova, Natàlia Plana, Vicent Ribas, Jordi Duran, Daniel Bach, Saadet Turkseven, Martine Laville, Hubert Vidal, Monika Karczewska-Kupczewska, Irina Kowalska, Marek Straczkowski, Xavier Testar, Manuel Palacín, Marco Sandri, Antonio L. Serrano, Antonio Zorzano.

Supplementary information includes nineteen figures, eight tables, supplementary methods and supplementary references.

Supplementary Figures

Figure S1

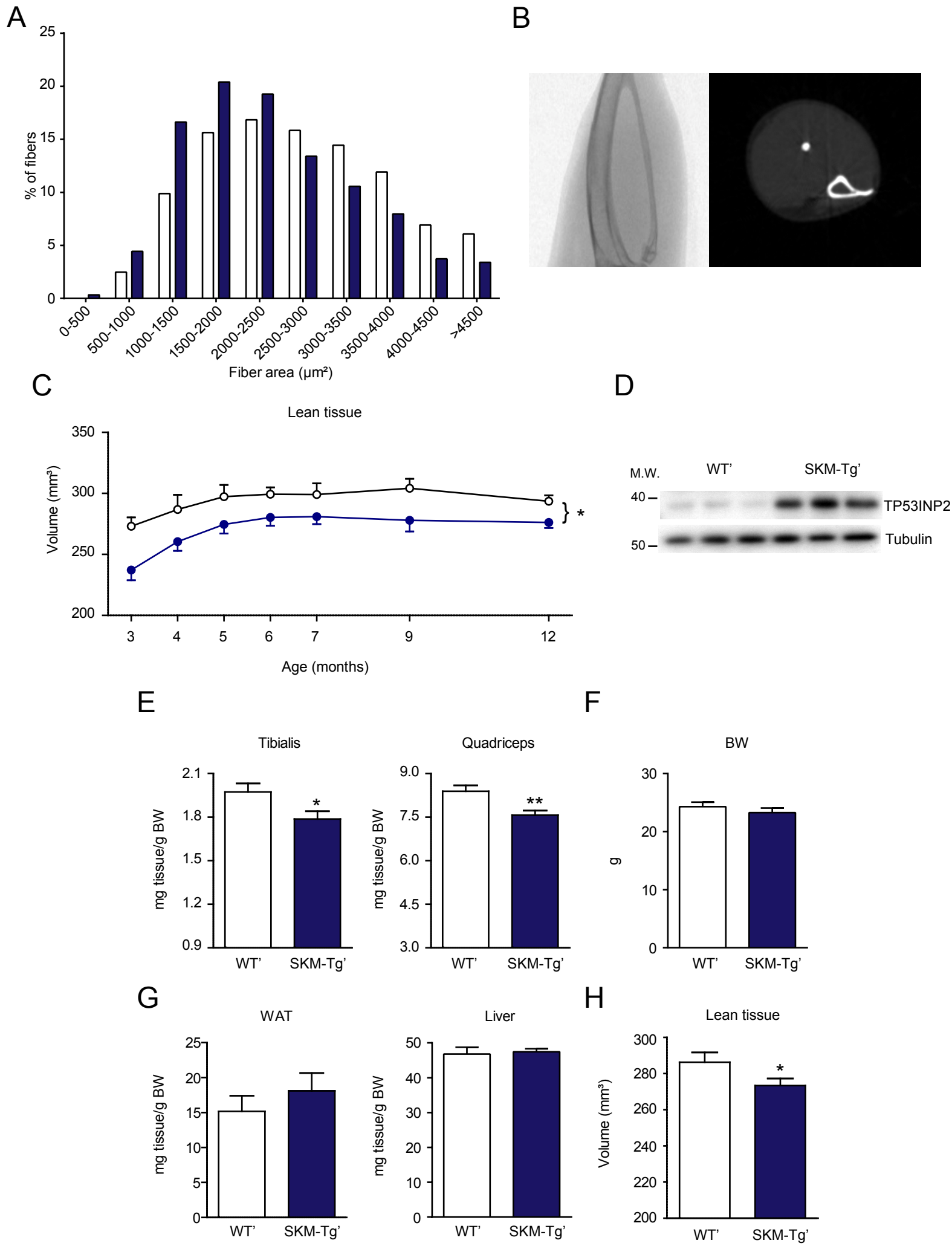
A
% of fibers
Fiber area (µm²)
0-500
500-1000
1000-1500
1500-2000
2000-2500
2500-3000
3000-3500
3500-4000
4000-4500
>4500
B
C
Lean tissue
Volume (mm³)
Age (months)
*
D
M.W.
WT'
SKM-Tg'
40
50
TP53INP2
Tubulin
E
Tibialis
Quadriceps
mg tissue/g BW
WT'
SKM-Tg'
F
BW
g
G
WAT
Liver
H
Lean tissue

Figure S1. A second transgenic mouse model with specific TP53INP2 gain-of-function in skeletal muscle (SMK-Tg') shows reduced muscle mass. (A) Muscle fiber distribution according to its cross-sectional area from tibialis anterior muscle from WT (white bars) and SKM-Tg mice (blue bars) (data were obtained from 6 WT and 6 SKM-Tg mice). (B) Images showing the region used to quantify the lean tissue volume. Left panel: Longitudinal section showing the region all along the entire fibula of the hindlimb of a mouse. Right panel: Transverse section in which the bone is clearly distinguished from the lean tissue. (C) Lean tissue volume of the right hindlimb of WT (white dots) and SKM-Tg mice (blue dots) from age 3 to 12 months (data were obtained in 8 WT and 9 SKM-Tg mice). (D) TP53INP2 protein levels in homogenates from quadriceps muscles of control (WT') and skeletal-muscle specific transgenic mice (SKM-Tg'). (E) Weights of tibialis anterior and quadriceps muscles from four-month-old WT' and SKM-Tg' mice. (F) Body weight of WT' and SKM-Tg' mice. (G) Epididymal adipose tissue and liver weights from WT' and SKM-Tg' mice. Data in panels E to G were obtained from 7 WT' and 8 SKM-Tg' mice. (H) Lean tissue volume of the right hindlimb of WT' and SKM-Tg' mice (data were obtained from 10 mice per group).

Data represent mean ± SEM. * $p<0.05$ and ** $p<0.01$ *vs* control mice.

Figure S2

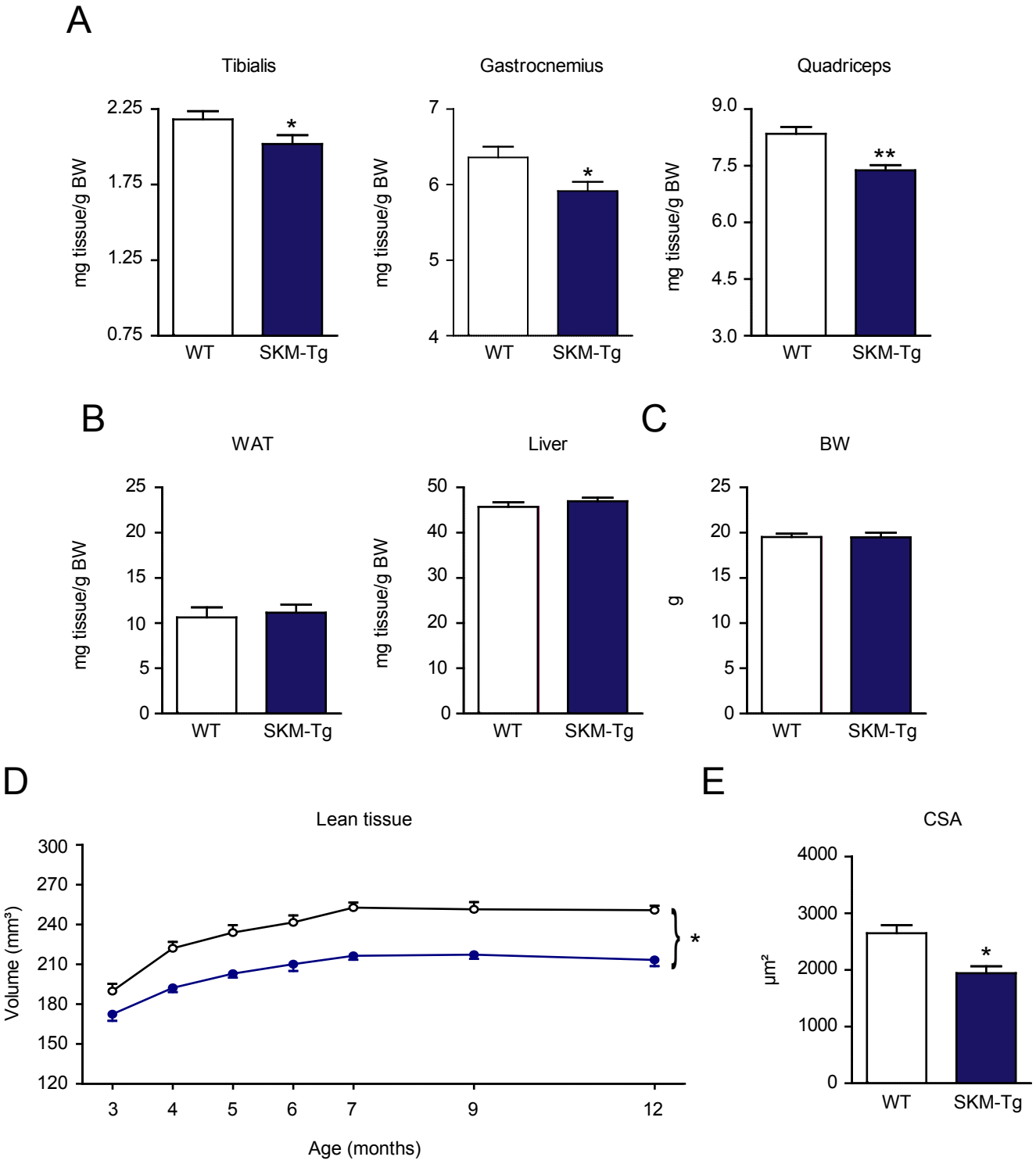
A
Tibialis
Gastrocnemius
Quadriceps
mg tissue/g BW
2.25
1.75
1.25
0.75
7
6
5
4
9.0
7.5
6.0
4.5
3.0
*
*
**
WT
SKM-Tg
B
WAT
Liver
C
BW
25
20
15
10
5
0
50
40
30
20
10
0
g
D
Lean tissue
Volume (mm³)
300
270
240
210
180
150
120
3
4
5
6
7
9
12
Age (months)
E
CSA
µm²
4000
3000
2000
1000
0

Figure S2. SKM-Tg females show reduced skeletal muscle mass. (A) Weights of tibialis anterior, gastrocnemius and quadriceps muscles from four-month-old WT and SKM-Tg mice. (B) Perigonadal white adipose tissue and liver weights from WT and SKM-Tg mice. (C) Body weight of WT and SKM-Tg mice. (D) Lean tissue volume of the right hindlimb of WT (white dots) and SKM-Tg mice (blue dots) from age 3 to the 12 months (data were obtained from 9 WT and 10 SKM-Tg mice). (E) Mean cross-sectional area (CSA) of 150 myofibers per each tibialis anterior muscle. Data in panels A to C and E were obtained from 8 WT and 8 SKM-Tg mice.

Data represent mean ± SEM. * $p<0.05$ and ** $p<0.01$ *vs* control mice.

Figure S3

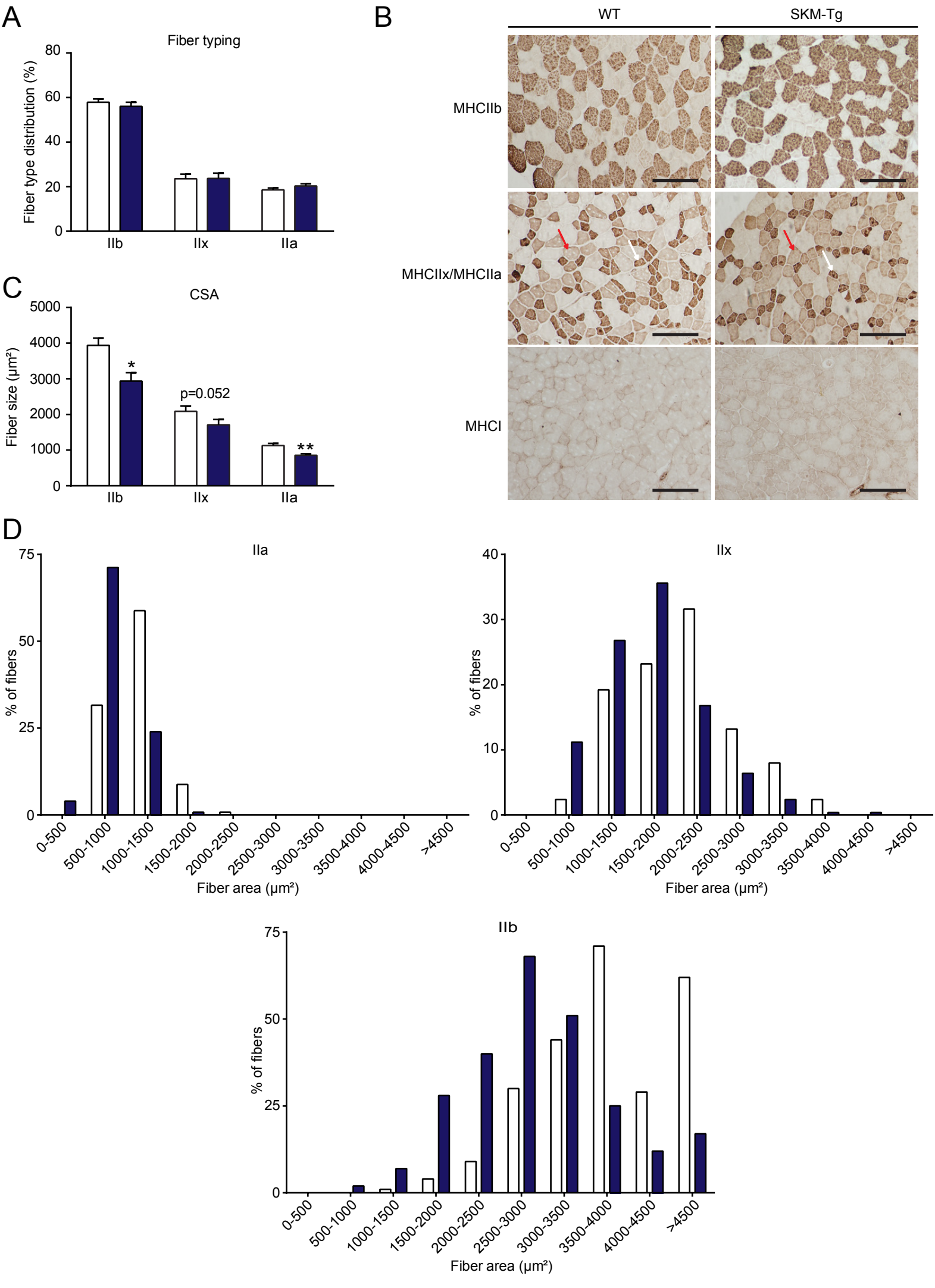
A
Fiber typing
Fiber type distribution (%)
80
60
40
20
0
IIb
IIx
IIa
B
WT
SKM-Tg
MHCIIb
MHCIIx/MHCIIa
MHCI
C
CSA
Fiber size (µm²)
5000
4000
3000
2000
1000
0
*
p=0.052
**
IIb
IIx
IIa
D
IIa
% of fibers
75
50
25
0
0-500
500-1000
1000-1500
1500-2000
2000-2500
2500-3000
3000-3500
3500-4000
4000-4500
>4500
Fiber area (µm²)
IIx
% of fibers
40
30
20
10
0
0-500
500-1000
1000-1500
1500-2000
2000-2500
2500-3000
3000-3500
3500-4000
4000-4500
>4500
Fiber area (µm²)
IIb
% of fibers
75
50
25
0
0-500
500-1000
1000-1500
1500-2000
2000-2500
2500-3000
3000-3500
3500-4000
4000-4500
>4500
Fiber area (µm²)

Figure S3. TP53INP2 reduces cross-sectional area from different fiber types without altering myofiber composition. Data were obtained from transversal sections of tibialis anterior muscle from 5 WT (white bars) and 5 SKM-Tg mice (blue bars). Cryosections were processed for immunohistochemistry for antibodies against MHC (myosin heavy chain) IIb, MHCIIx and MHCIIa, and MHCI. (A) Muscle fiber composition, (B) Representative images, (C) mean cross-sectional area and (D) distribution according to the cross-sectional area from different fiber types is shown. Red arrows point to representative MHCIIx myofibers. White arrows point to representative MHCIIa myofibers. Scale bar, 200 μm. No MHCI signal was found in tibialis anterior muscles from WT or SKM-Tg mice.

Data represent mean ± SEM. * $p<0.05$ and ** $p<0.01$ *vs* control mice.

Figure S4

A

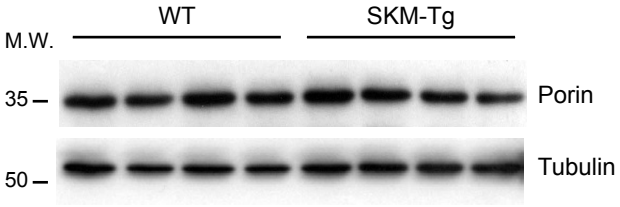
WT
SKM-Tg
M.W.
35
50
Porin
Tubulin

B

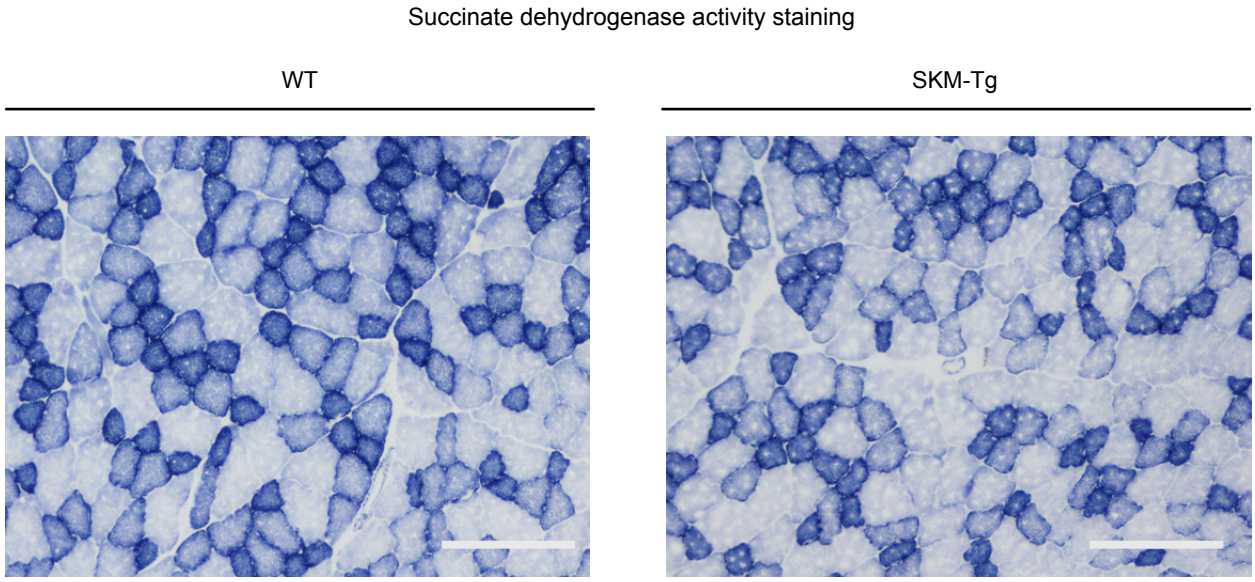
Succinate dehydrogenase activity staining
WT
SKM-Tg

Figure S4. SKM-Tg mice do not show alterations in mitochondrial content or functionality. (A) Porin protein levels in homogenates from quadriceps muscles from WT and SKM-Tg mice. (B) Representative images of succinate dehydrogenase staining from transverse sections of quadriceps muscles from WT and SKM-Tg animals. Scale bar, 200 μm.

Figure S5

A

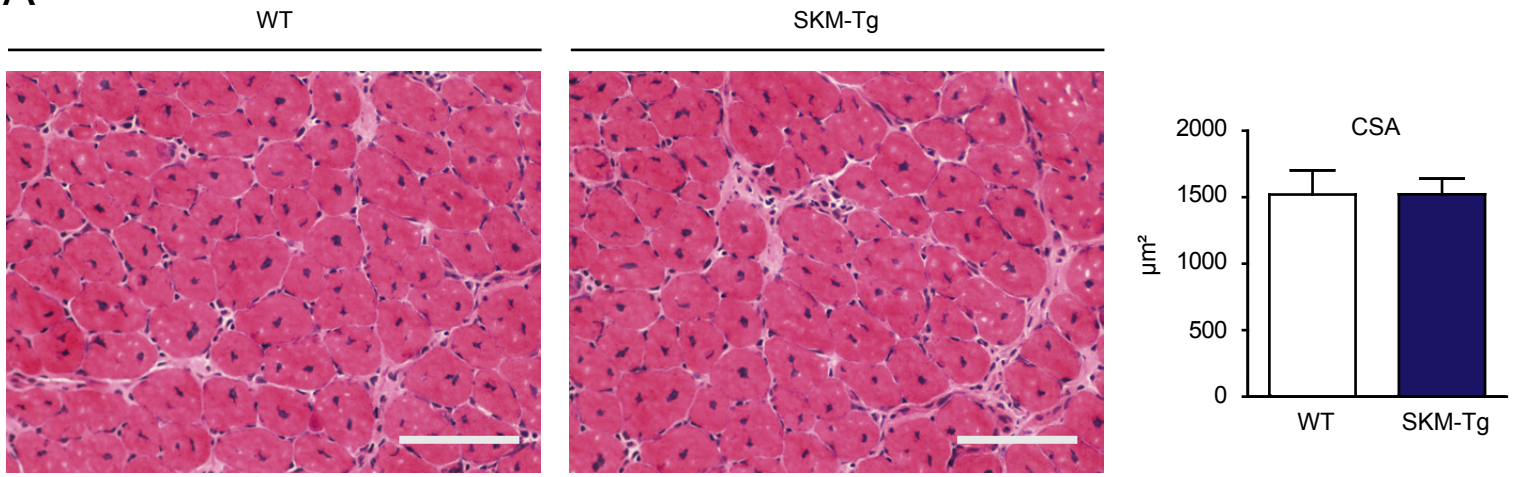
WT
SKM-Tg
CSA
2000
1500
1000
500
0
µm²
WT
SKM-Tg

B

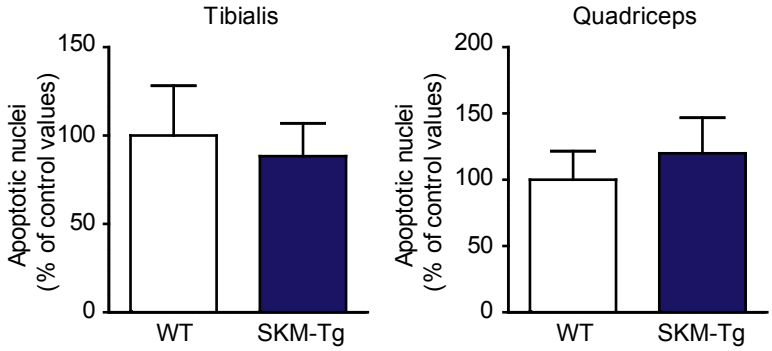
Tibialis
Quadriceps
Apoptotic nuclei
(% of control values)
150
100
50
0
200
150
100
50
0
WT
SKM-Tg
WT
SKM-Tg

Figure S5. SKM-Tg mice do not show alterations in the early steps of the regeneration process or in the number of apoptotic nuclei. (A) Left panels: Representative images of haematoxylin and eosin staining from regenerating tibialis anterior muscles from WT and SKM-Tg animals 7 days post-injury. Newly formed myofibers can be distinguished by the centrally located nuclei. Scale bar, 100 μm. Right panel: Mean cross-sectional area (CSA) of 150 myofibers per tibialis anterior muscles from WT and SKM-Tg mice. (B) Number of apoptotic nuclei assessed by TUNEL in transverse sections of tibialis anterior and quadriceps muscles from WT and SKM-Tg animals.

Data represent mean ± SEM (8 mice per group were used in regeneration studies and 10 in TUNEL assays).

Figure S6

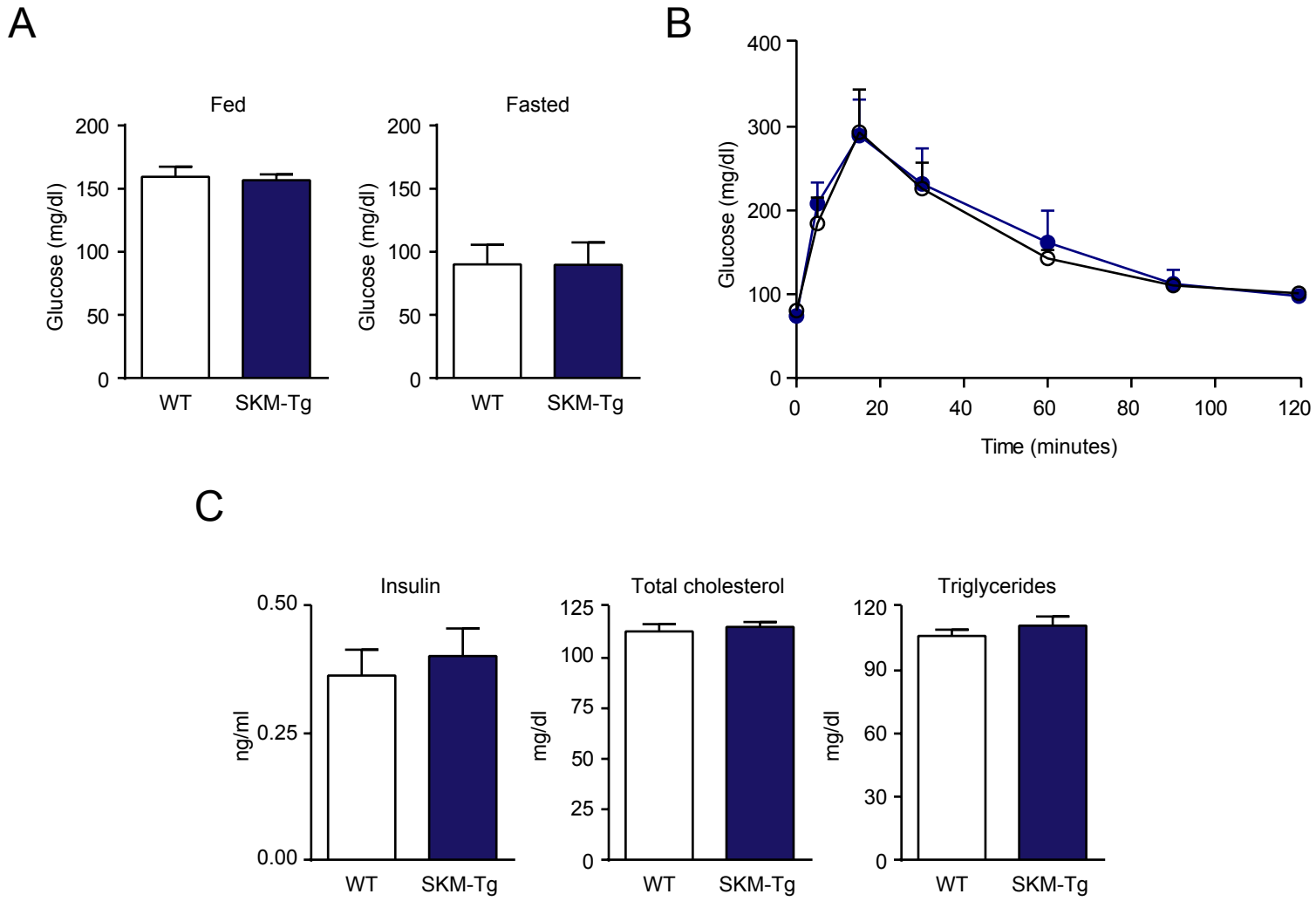
A
Fed
Fasted
Glucose (mg/dl)
200
150
100
50
0
WT
SKM-Tg
B
400
300
200
100
0
0
20
40
60
80
100
120
Time (minutes)
C
Insulin
ng/ml
0.50
0.25
0.00
Total cholesterol
mg/dl
125
100
75
50
25
Triglycerides
120
90
60
30

Figure S6. TP53INP2 gain-of-function in skeletal muscle does not alter glucose metabolism. (A) Glucose blood levels in fed or 16 h fasted WT and SKM-Tg mice (data were obtained in 8 mice per group). (B) Glucose tolerance test on WT and SKM-Tg mice (data were obtained in 5 mice per group). (C) Insulin, total cholesterol and triglycerides plasma levels from 16 h fasted WT and SKM-Tg mice (data were obtained in 11 mice per group).

Data represent mean ± SEM.

Figure S7

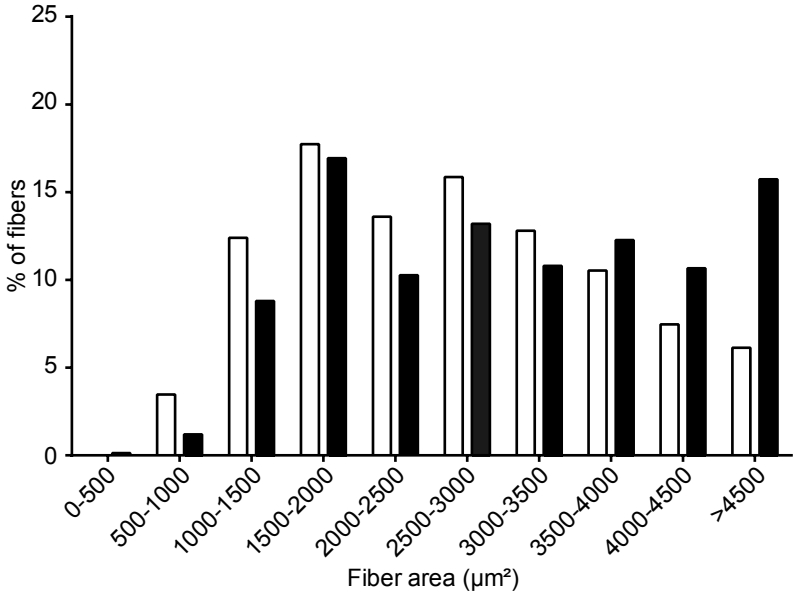
25
20
15
10
5
0
% of fibers
0-500
500-1000
1000-1500
1500-2000
2000-2500
2500-3000
3000-3500
3500-4000
4000-4500
>4500
Fiber area (µm²)

Figure S7. SKM-KO mice show and increase in myofiber cross-sectional area. Muscle fiber distribution according to its cross-sectional area from tibialis anterior muscle from C (white bars) and SKM-KO mice (black bars) (data were obtained from 6 C and 10 SKM-KO mice).

Figure S8

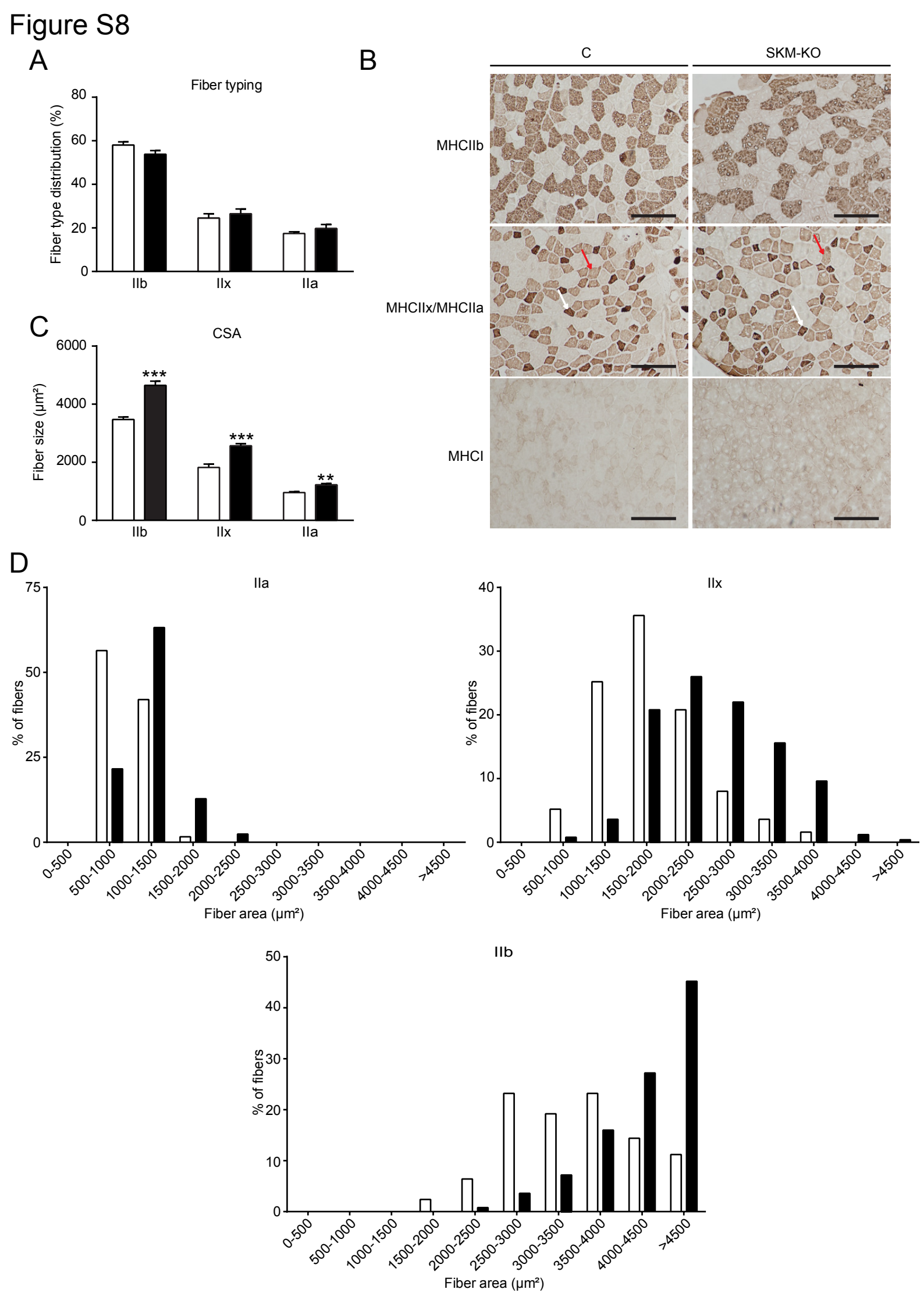
A
Fiber typing
Fiber type distribution (%)
80
60
40
20
0
IIb
IIx
IIa
B
C
SKM-KO
MHCIIb
MHCIIx/MHCIIa
MHCI
C
CSA
Fiber size (µm²)
6000
4000
2000
0
***
***
**
IIb
IIx
IIa
D
IIa
% of fibers
75
50
25
0
0-500
500-1000
1000-1500
1500-2000
2000-2500
2500-3000
3000-3500
3500-4000
4000-4500
>4500
Fiber area (µm²)
IIx
% of fibers
40
30
20
10
0
0-500
500-1000
1000-1500
1500-2000
2000-2500
2500-3000
3000-3500
3500-4000
4000-4500
>4500
Fiber area (µm²)
IIb
% of fibers
50
40
30
20
10
0
0-500
500-1000
1000-1500
1500-2000
2000-2500
2500-3000
3000-3500
3500-4000
4000-4500
>4500
Fiber area (µm²)

Figure S8. TP53INP2 ablation increases cross-sectional area from different fiber types without altering myofiber composition. Data were obtained from transversal sections of tibialis anterior muscle from 5 C (white bars) and 5 SKM-KO mice (black bars). Cryosections were processed for immunohistochemistry for antibodies against MHC (myosin heavy chain) IIb, MHCIIx and MHCIIa, and MHCI. (A) Muscle fiber composition, (B) Representative images, (C) mean cross-sectional area and (D) distribution according to the cross-sectional area from different fiber types is shown. Red arrows point to representative MHCIIx myofibers. White arrows point to representative MHCIIa myofibers. Scale bar, 200 μm. No MHCI signal was found in tibialis anterior muscles from C or SKM-KO mice.

Data represent mean ± SEM. ** $p<0.01$ and *** $p<0.001$ *vs* control mice.

Figure S9

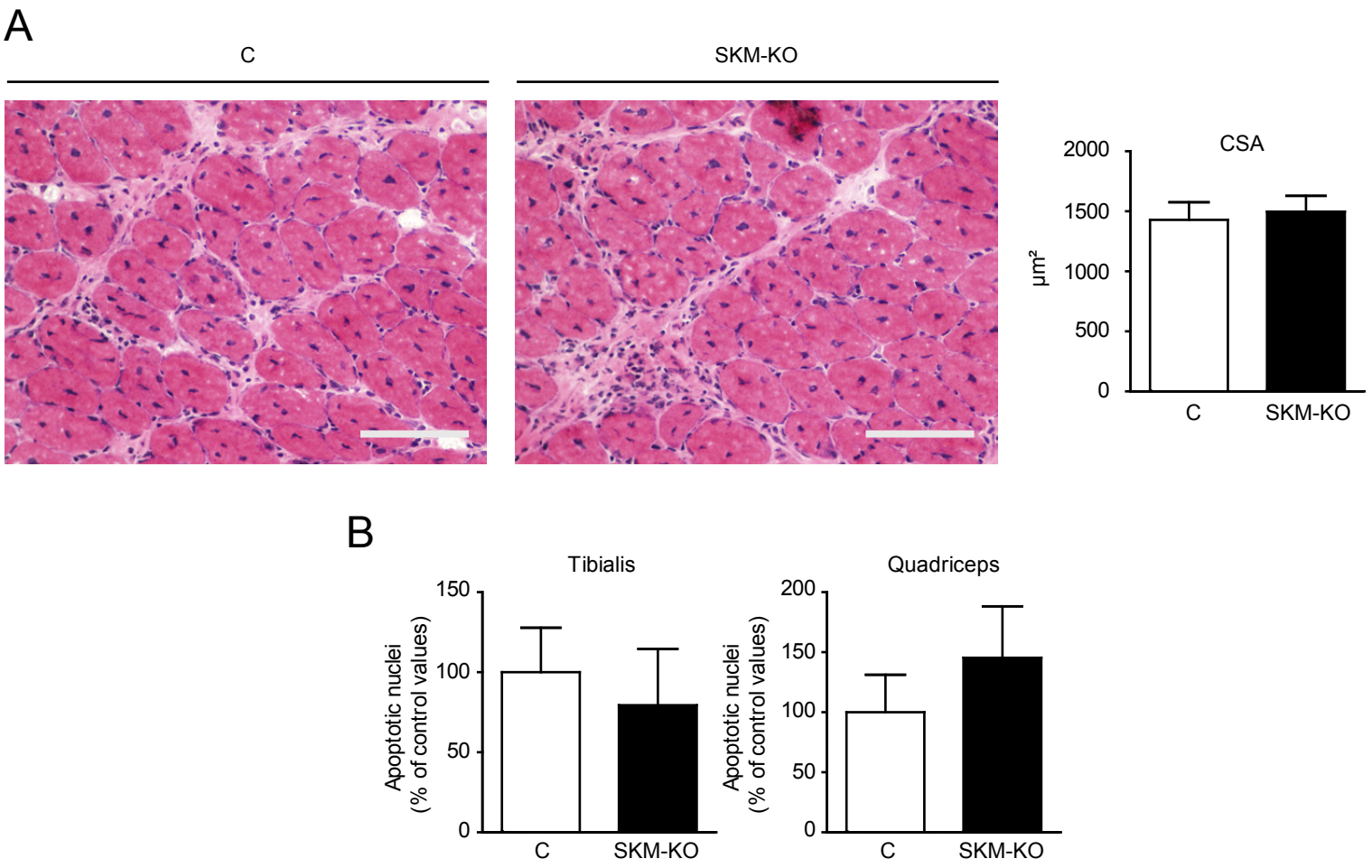
A
C
SKM-KO
CSA
2000
1500
1000
500
0
µm²
C
SKM-KO
B
Tibialis
Quadriceps
Apoptotic nuclei
(% of control values)
150
100
50
0
200
150
100
50
0
C
SKM-KO
C
SKM-KO

Figure S9. SKM-KO mice do not show alterations in the early steps of the regeneration process or in the number of apoptotic nuclei. (A) Left panels: Representative images of haematoxylin and eosin staining from regenerating tibialis anterior muscles from C and SKM-KO animals 7 days post-injury. Newly formed myofibers can be distinguished by the centrally located nuclei. Scale bar, 100 μm. Right panel: Mean cross-sectional area (CSA) of 150 myofibers per tibialis anterior muscles from C and SKM-KO mice (data were obtained from 8 mice per group). (B) Number of apoptotic nuclei assessed by TUNEL in transverse sections of tibialis anterior and quadriceps muscles from C and SKM-KO animals (data were obtained from 10 mice per group).

Data represent mean ± SEM.

Figure S10

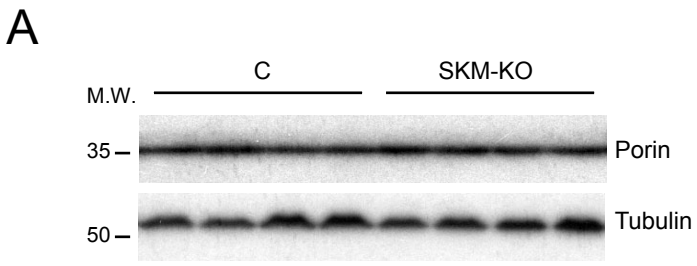
A
C
SKM-KO
M.W.
35
Porin
50
Tubulin

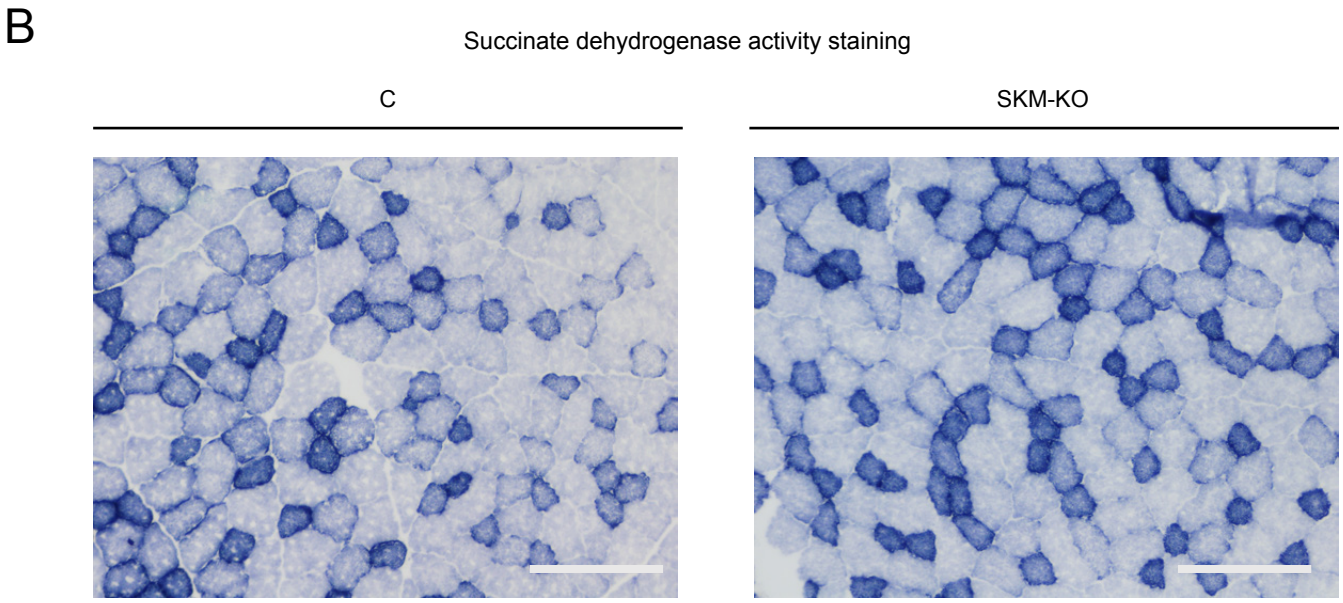
B
Succinate dehydrogenase activity staining
C
SKM-KO

Figure S10. SKM-KO mice do not show alterations in mitochondrial content and functionality. (A) Porin protein levels in homogenates from quadriceps muscles from C and SKM-KO animals. (B) Representatives images of succinate dehydrogenase staining from transverse sections of quadriceps muscles from C and SKM-KO mice. Scale bar, 200 μm.

Figure S11

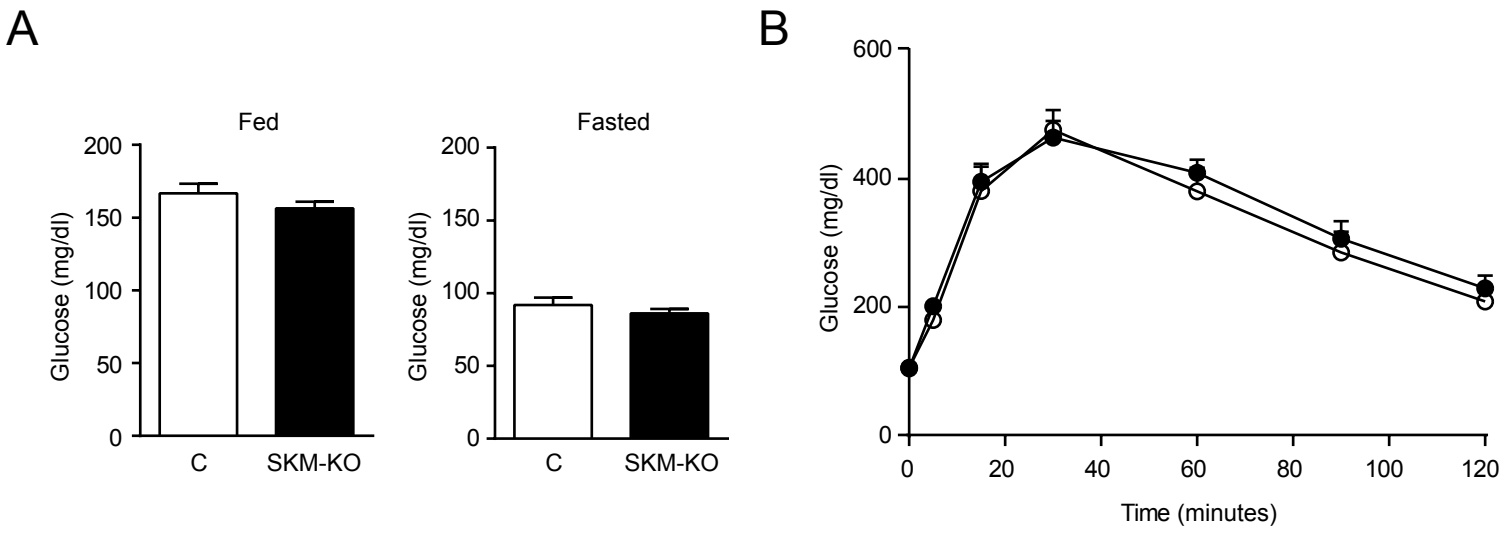
A
Fed
Fasted
Glucose (mg/dl)
200
150
100
50
0
C
SKM-KO
B
600
400
200
0
0
20
40
60
80
100
120
Time (minutes)

Figure S11. TP53INP2 ablation in skeletal muscle does not alter glucose metabolism. (A) Glucose blood levels in fed or 16 h fasted C and SKM-KO mice (data were obtained in 15 mice per group). (B) Glucose tolerance test on C and SKM-KO mice (data were obtained from 6 mice per group).

Data represent mean ± SEM.

Figure S12

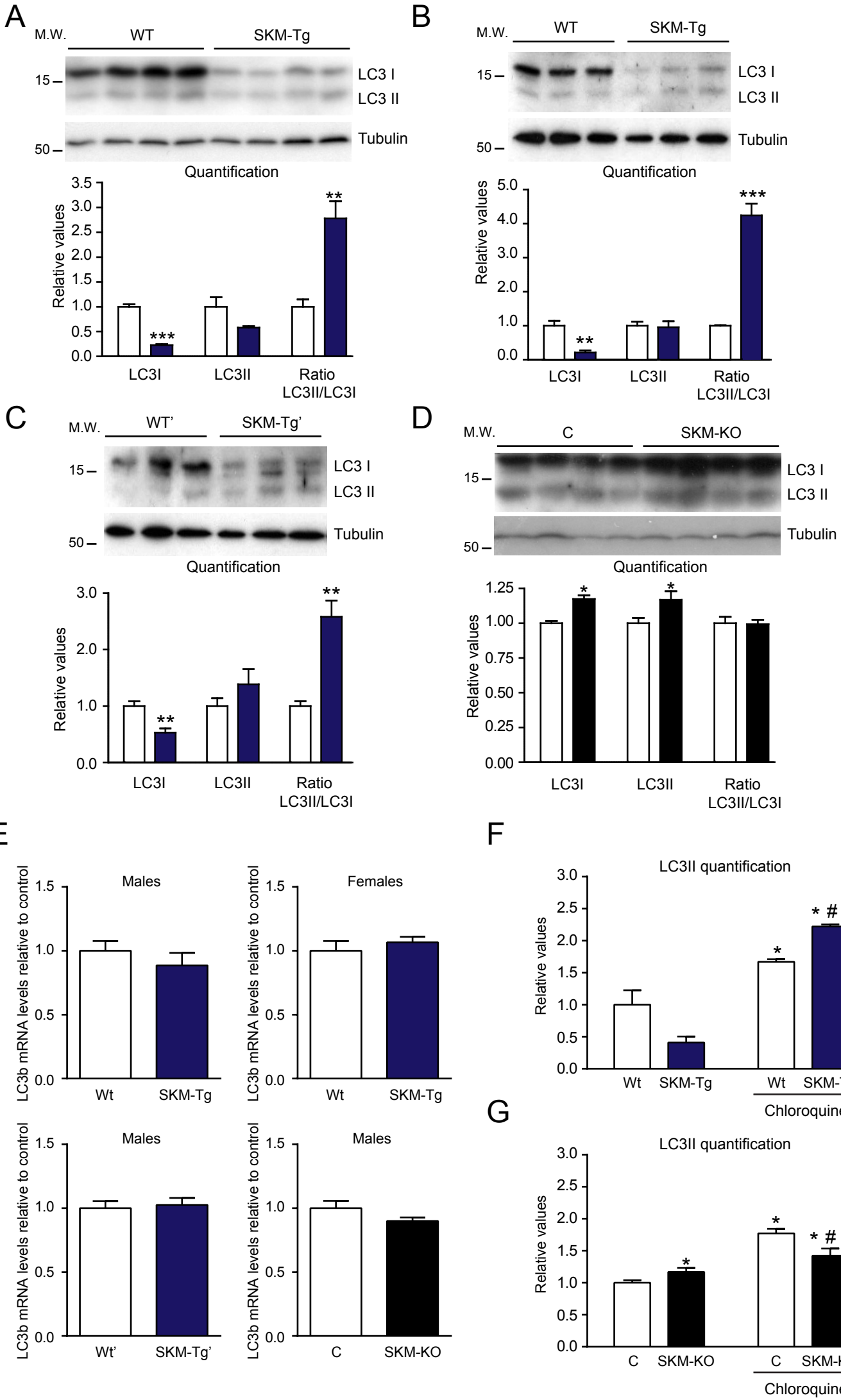
A
M.W.
WT
SKM-Tg
15
LC3 I
LC3 II
50
Tubulin
Quantification
Relative values
LC3I
LC3II
Ratio LC3II/LC3I
B
C
WT'
SKM-Tg'
D
C
SKM-KO
E
Males
Females
LC3b mRNA levels relative to control
Wt
SKM-Tg
Wt'
SKM-Tg'
C
SKM-KO
F
LC3II quantification
Chloroquine
G

Figure S12. TP53INP2 gain-of-function activates autophagy in SKM-Tg female mice and in a second transgenic line (SKM-Tg'). Panels A-C: Western blot analysis of LC3I and LC3II in total homogenates of gastrocnemius muscles from (A) four-month-old WT (white bars) and SKM-Tg (blue bars) male mice, (B) four-month-old WT (white bars) and SKM-Tg (blue bars) female mice or (C) four-month-old WT' (white bars) and SKM-Tg' (blue bars) male mice. Top panels: Representative images. Bottom panels: Quantification (n=5). (D) Western blot analysis of LC3I and LC3II protein levels in total homogenates of gastrocnemius muscles from C (white bars) and SKM-KO male mice (black bars). Top panel: Representative images. Bottom panel: Quantification (n=5). (E) LC3b mRNA levels measured in quadriceps muscle from WT and SKM-Tg males (n=7), WT and SKM-Tg females (n=7), WT' and SKM-Tg' males (n=5) and C and SKM-KO males (n=10). Panels F-G: Quantification of LC3II protein levels in total homogenates of gastrocnemius muscles from (F) WT and SKM-Tg mice (n=5) or (G) C and SKM-KO mice (n=5) with or without chloroquine treatment. These quantifications refer to the western blots shown in Figure 3A.

Data represent mean ± SEM. * $p<0.05$ and ** $p<0.01$ *vs* control mice; # $p<0.05$ *vs* SKM-Tg or SKM-KO mice; & $p<0.05$ *vs* treated WT or C mice.

Figure S13

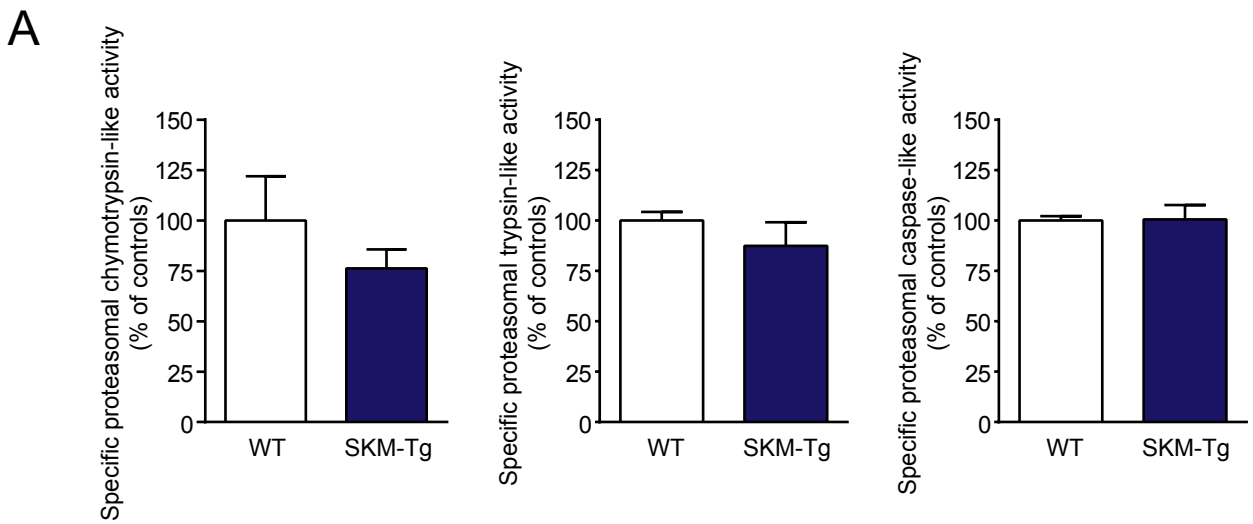
A
Specific proteasomal chymotrypsin-like activity (% of controls)
150
125
100
75
50
25
0
WT
SKM-Tg
Specific proteasomal trypsin-like activity (% of controls)
150
125
100
75
50
25
0
WT
SKM-Tg
Specific proteasomal caspase-like activity (% of controls)
150
125
100
75
50
25
0
WT
SKM-Tg

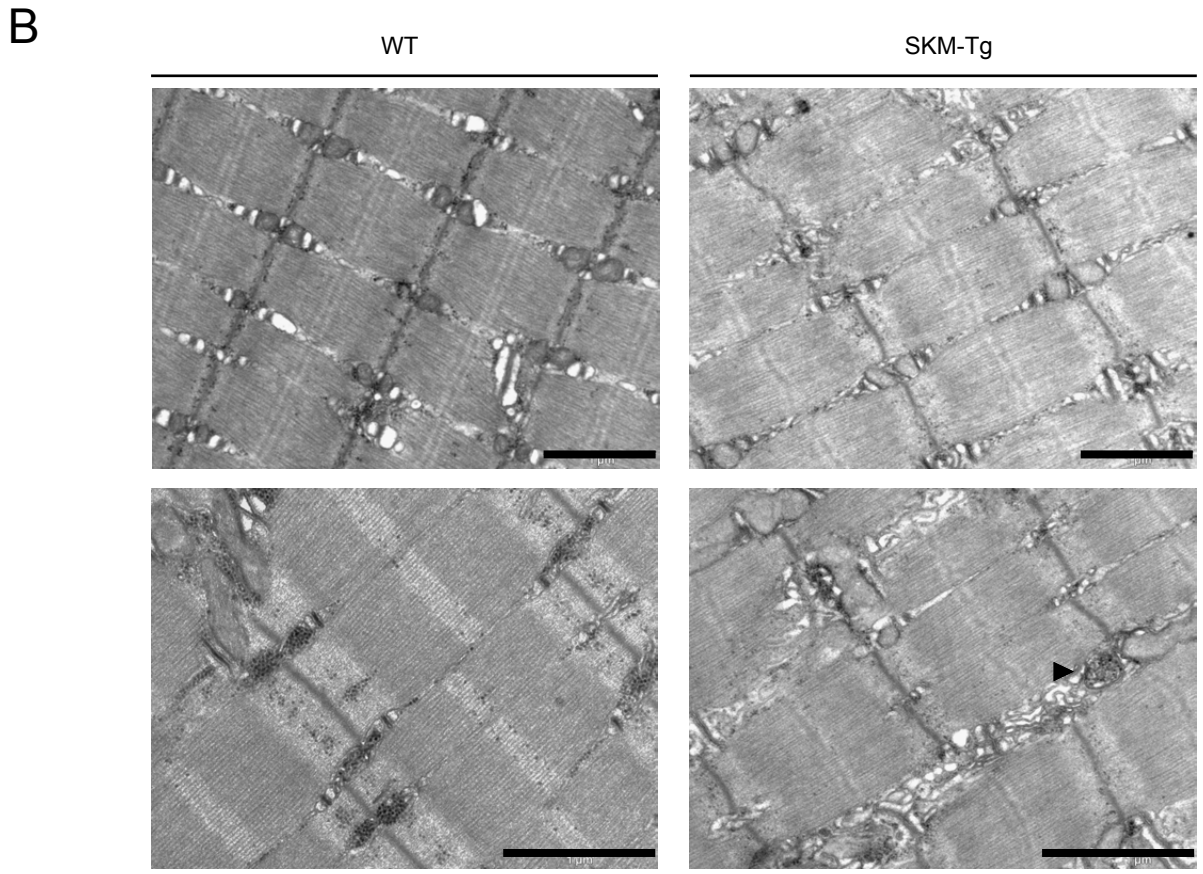
B
WT
SKM-Tg


C
a
b
c

Figure S13. SKM-Tg mice do not display changes in proteasome activity or in muscle ultrastructure. (A) Mean specific chymotrypsin-like, trypsin-like and caspase-like proteasomal activity in total extracts of EDL muscle from WT and SKM-Tg mice (n=5). (B) Representative electron microscopy images from quadriceps muscles from WT and SKM-Tg mice. Arrows indicate autophagosome-related structures. Scale bar, 1 μm. (C) Electron microscopy images showing autophagosome-related structures from quadriceps muscles of SKM-Tg mice. Scale bar, 500 nm (a and b) and 200 nm (c).

Data represent mean ± SEM.

Figure S14

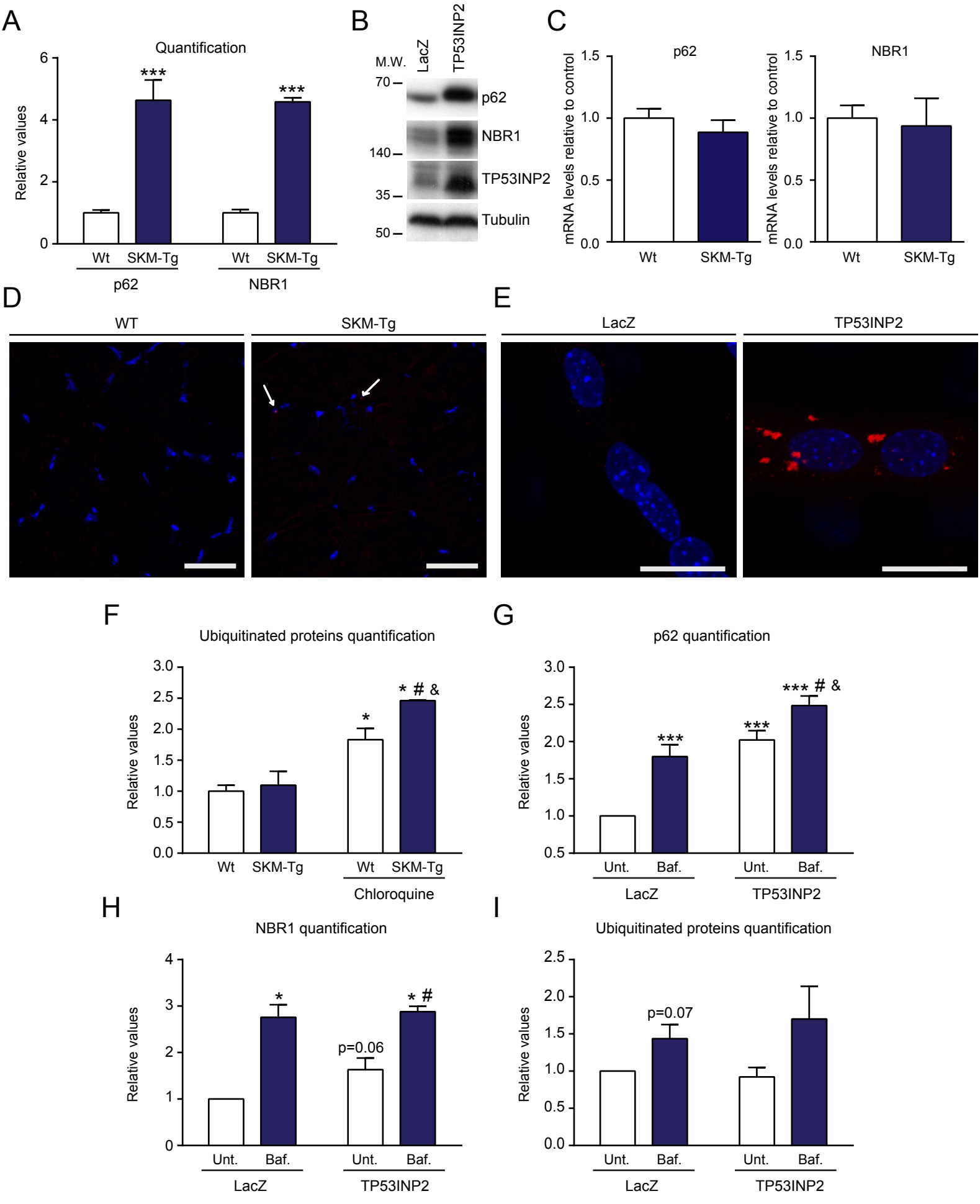
A
Quantification
Relative values
***
***
Wt
SKM-Tg
Wt
SKM-Tg
p62
NBR1
B
M.W.
LacZ
TP53INP2
70
140
35
50
p62
NBR1
TP53INP2
Tubulin
C
p62
NBR1
mRNA levels relative to control
Wt
SKM-Tg
D
WT
SKM-Tg
E
LacZ
TP53INP2
F
Ubiquitinated proteins quantification
Relative values
Wt
SKM-Tg
Wt
SKM-Tg
Chloroquine
G
p62 quantification
Relative values
Unt.
Baf.
LacZ
TP53INP2
H
NBR1 quantification
Relative values
p=0.06
I
Ubiquitinated proteins quantification
Relative values
p=0.07

Figure S14. TP53INP2 overexpression causes the accumulation of p62. (A) Quantification of p62 and NBR1 protein levels in total homogenates of gastrocnemius muscles from WT and SKM-Tg male mice (n=5). This quantification refers to the western blot shown in Figure 4A. (B) p62, NBR1 and TP53INP2 levels in protein extracts from C2C12 myotubes infected with adenovirus coding for TP53INP2 or LacZ (control). (C) p62 and NBR1 mRNA levels measured in quadriceps muscle from WT and SKM-Tg mice (n=7). Panels D-E: Representative images of p62 immunofluorescence in (D) transversal sections of tiabialis anterior muscles from four-month-old WT and SKM-Tg mice or in (E) control (LacZ) and TP53INP2 overexpressing C2C12 myotubes. p62 is shown in red and nuclei in blue (Hoechst33342 staining). Scale bar, 40 μm (for C) and 20 μm (for D). (F) Quantification of ubiquitinated protein content in total homogenates of gastrocnemius muscles from WT and SKM-Tg mice with or without chloroquine treatment (n=5). This quantification refers to the western blot shown in Figure 4B. Panels G-I: Quantification of p62, NBR1 and TP53INP2 levels in protein extracts from C2C12 myotubes infected with adenovirus coding for TP53INP2 or LacZ (control). Cells were treated with bafilomycin A1 for 3h when indicated. This quantifications refer to the western blot shown in Figure 4C.

Data represent mean ± SEM. * $p<0.05$, ** $p<0.01$ and *** $p<0.001$ *vs* control conditions; # $p<0.05$ *vs* SKM-Tg mice or TP53INP2 overexpressing myotubes; & $p<0.05$ *vs* treated WT mice or LacZ bafilomycin treated myotubes.

Figure S15

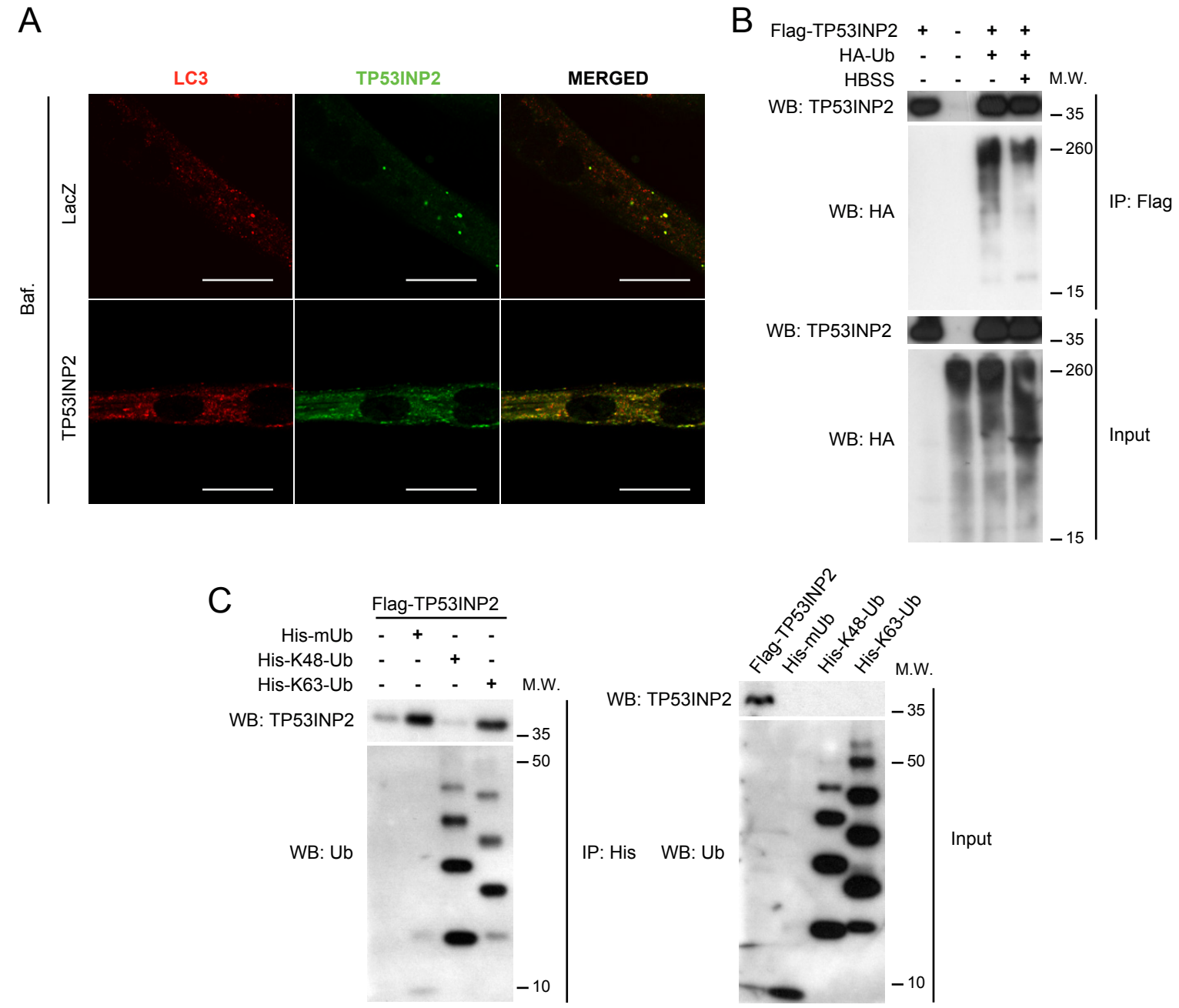
A
LC3
TP53INP2
MERGED
Baf.
LacZ
TP53INP2
B
Flag-TP53INP2
HA-Ub
HBSS
M.W.
WB: TP53INP2
WB: HA
IP: Flag
Input
35
260
15
C
Flag-TP53INP2
His-mUb
His-K48-Ub
His-K63-Ub
WB: TP53INP2
WB: Ub
IP: His
50
10

Figure S15. TP53INP2 overexpression displaces p62 from autophagosomes and interacts with ubiquitin. (A) Immunofluorescence against LC3 and TP53INP2 in control (LacZ) and TP53INP2 overexpressing C2C12 myotubes (day 5). Cells were treated with bafilomycin A1 at 200 nM during 3h. LC3 is stained in red and TP53INP2 in green. Scale bar, 20 μm. (B) HEK 293T cells were transfected with plasmids coding for Flag-mTP53INP2 and/or HA-Ub. Where indicated, 2h of starvation was induced by incubating cells with HBSS media. Pull-down assays were performed using Flag resin and inputs and pellets were probed in Western blot assays with anti-TP53INP2 and anti-HA antibodies. (C) Cobalt resin coupled to recombinant His-tagged mono-Ub, K48-Ub and K63-Ub was incubated with Flag-TP53INP2 previously pulled down using Flag-resin. Inputs and elutions of the proteins attached to the cobalt resin were proved in Western blot assays with anti-Ub (FK2) and anti-TP53INP2 antibodies.

Figure S16

A

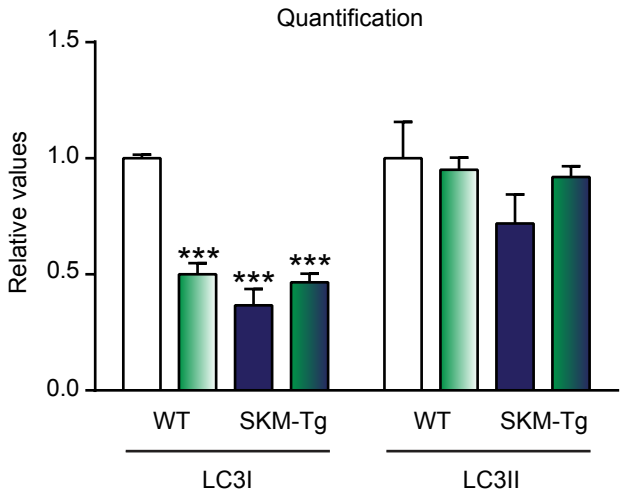

B

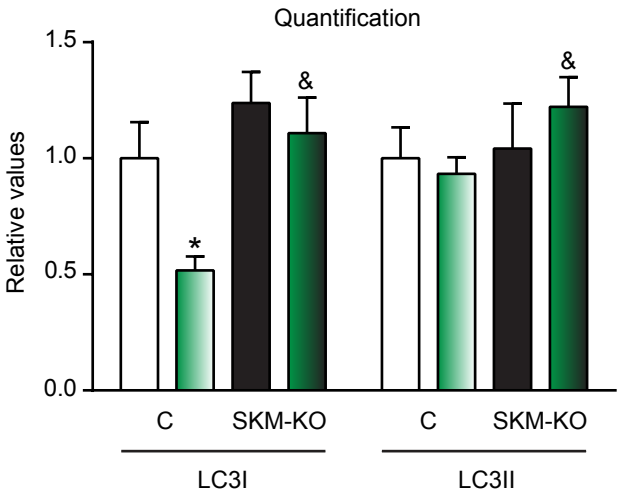

Figure S16. Autophagy is activated by streptozotocin-induced diabetes. Panels A and B: Quantification of LC3I and LC3II protein levels in total homogenates of gastrocnemius muscles from (A) WT and SKM-Tg male mice or (B) C and SKM-KO male mice treated or not with streptozotocin (n=5). These quantifications refer to the western blots shown in Figure 5I and 5J respectively. White bars refer to WT or C mice; blue bars to SKM-Tg animals; and black bars to SKM-KO mice. The green colour indicates mice treated with streptozotocin.

Data represent mean ± SEM. *** $p<0.001$ *vs* control mice; & $p<0.05$ *vs* diabetic C mice.

Figure S17

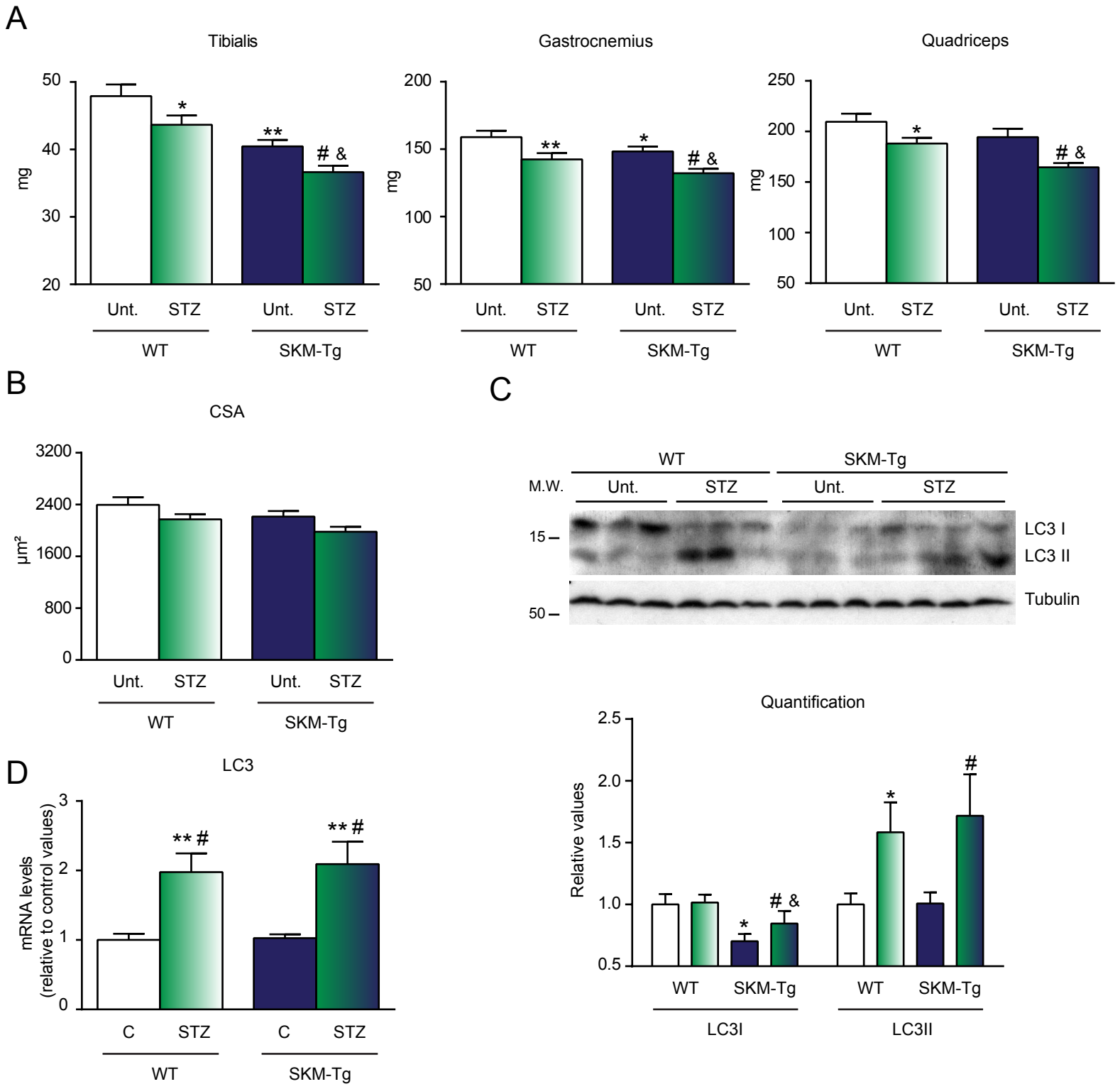
A
Tibialis
Gastrocnemius
Quadriceps
mg
Unt.
STZ
WT
SKM-Tg
B
CSA
µm²
C
WT
SKM-Tg
M.W.
LC3 I
LC3 II
Tubulin
Quantification
Relative values
LC3I
LC3II
D
LC3
mRNA levels
(relative to control values)
C

Figure S17. Autophagy blockage blunts TP53INP2 effect on diabetes induced muscle wasting. Panel A-B: (A) Weights of tibialis anterior, gastrocnemius and quadriceps muscles and (B) mean cross-sectional area (CSA) of 150 myofibers per tibial from chloroquine treated WT and SKM-Tg mice injected or not with streptozotocin (STZ). (C) Western blot analysis of LC3I and LC3II content in total homogenates of gastrocnemius muscles from chloroquine treated WT and SKM-Tg injected or not with streptozotocin (STZ). Upper panel: Representative images. Lower panel: Quantification (n=5). (D) LC3b mRNA levels measured in quadriceps muscles from WT and SKM-Tg mice with or without streptozotocin treatment (n=7)

Data represent mean ± SEM. Data in panel A were obtained from 6 non-diabetic WT, 6 non-diabetic SKM-Tg, 8 STZ treated WT and 7 STZ treated SKM-Tg mice. Data in panels B were obtained from 5 animals per group. * $p<0.05$ and ** $p<0.01$ *vs* non-diabetic WT mice; # $p<0.05$ *vs* non-diabetic SKM-Tg mice; & $p<0.05$ *vs* diabetic WT mice.

Figure S18

A

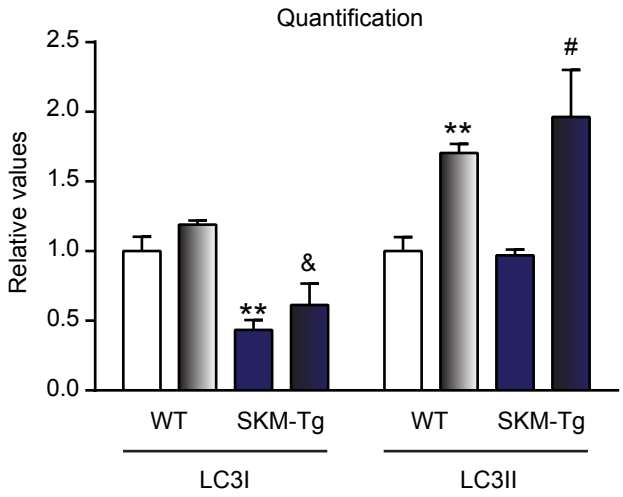

B

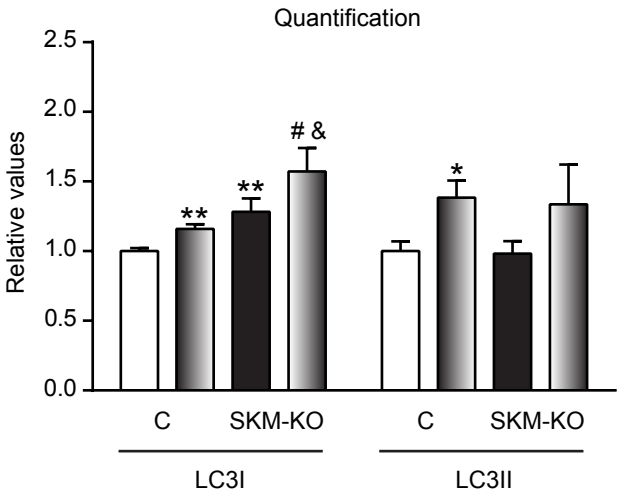

Figure S18. Autophagy is blocked under denervation conditions. Panels A and B: Quantification of LC3I and LC3II protein levels in total homogenates of gastrocnemius muscles from (A) WT and SKM-Tg male mice or (B) C and SKM-KO male mice (n=5). Sciatic nerve from right hindlimb was transected and left hindlimb was used as control. This quantifications refer to the western blots shown in Figure 6F and 6G respectively. White bars refer to WT or C mice; blue bars to SKM-Tg animals; and black bars to SKM-KO mice. The grey colour indicates data from denervated hindlimbs.

Data represent mean ± SEM. * $p<0.05$ and ** $p<0.01$ *vs* control mice; # $p<0.05$ *vs* control SKM-Tg or SKM-KO mice; & $p<0.01$ *vs* denervated control mice.

Figure S19

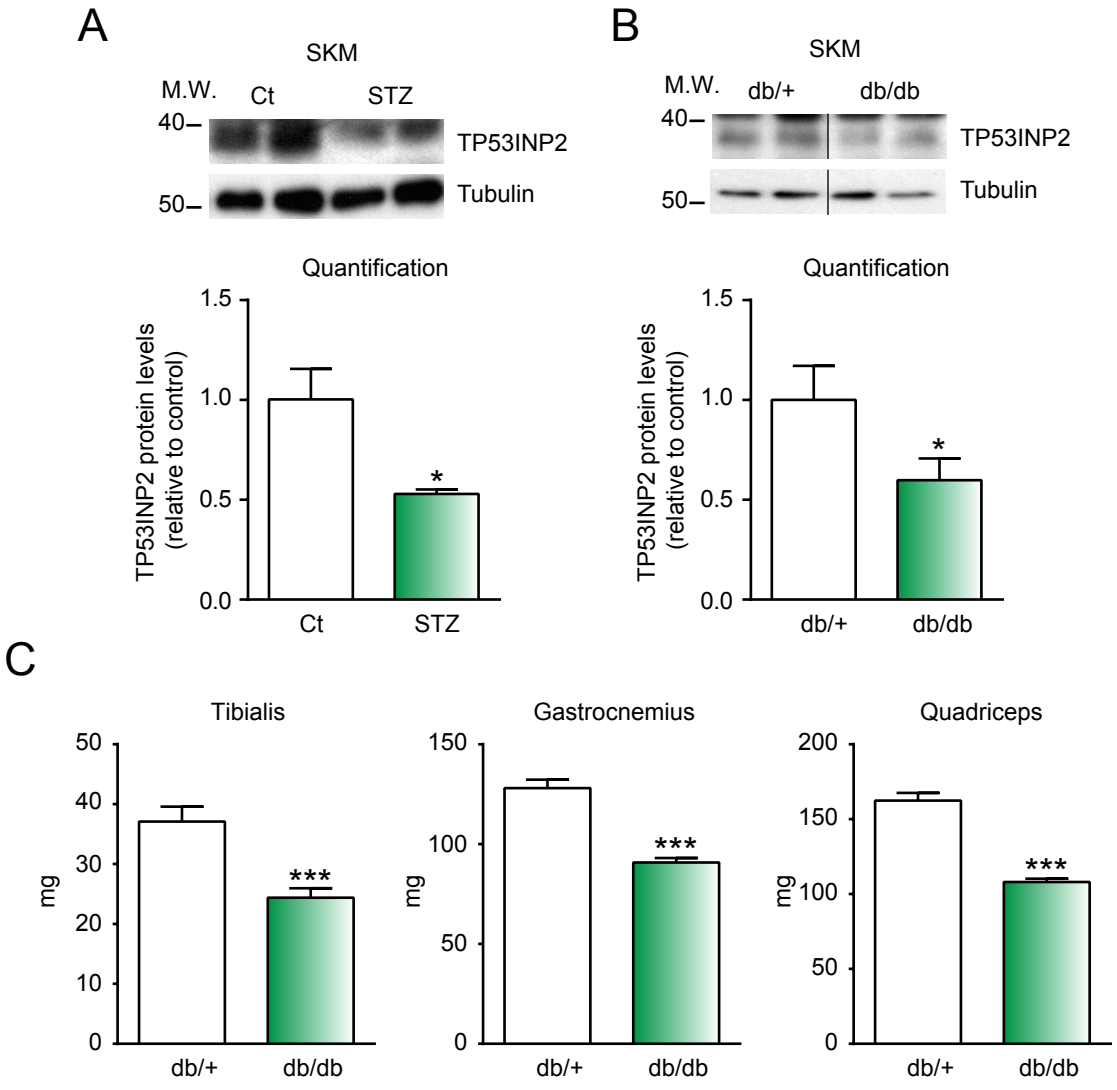
A
SKM
M.W.
Ct
STZ
40
50
TP53INP2
Tubulin
Quantification
TP53INP2 protein levels (relative to control)
1.5
1.0
0.5
0.0
*
Ct
STZ
B
SKM
M.W.
db/+
db/db
40
50
TP53INP2
Tubulin
Quantification
TP53INP2 protein levels (relative to control)
1.5
1.0
0.5
0.0
*
db/+
db/db
C
Tibialis
mg
50
40
30
20
10
0
***
db/+
db/db
Gastrocnemius
mg
150
100
50
0
***
db/+
db/db
Quadriceps
mg
200
150
100
50
0
***
db/+
db/db

Figure S19. TP53INP2 is repressed in skeletal muscle from murine models of diabetes. Panels A-B: Western blot analysis of TP53INP2 protein content in homogenates of quadriceps muscles from (A) control and 5 days streptozotocin-induced diabetic mice or (B) lean ten-weeks-old (db/+) and db/db mice. Upper panels: Representative images. Thin black lines indicate that lanes were run on the same gel but were non-contiguous. Lower panels: Quantifications (n=5). (C) Weights of tibialis anterior, gastrocnemius and quadriceps muscles from lean (db/+) and db/db mice (n=5).

Data represent mean ± SEM. * $p<0.05$ and *** $p<0.001$ *vs* control mice.

Supplementary Methods

Plasmids

The following plasmids were used for *in vivo* gene transfer experiments: mTP53INP2-RFP (1) (generated in our laboratory) and EGFP-LC3 (2) (Guido Kroemer, INSERM, Institut Gustave Roussy and Université Paris Sud, Villejuif, France).

For immunoprecipitation assays, the following plasmids were used: mTP53INP2 (3) (generated in our laboratory), Flag-mTP53INP2 (generated in our laboratory), mTP53INP2 3KR (generated in our laboratory), GFP-Ub (4) (Jacques Neefjes, The Netherlands Cancer Institute, Amsterdam, Netherlands), HA-Ub (5) (Edward T. H. Yeh, The University of Texas-Huston Health Science Center, Huston, USA), His-monoUb (Boston Biochem, Inc.), His-Ub48 (Boston Biochem, Inc.), His-Ub63 (Boston Biochem, Inc.).

Subjects

For RNA expression assays, vastus lateralis muscle samples from Lyon were obtained during previous published studies (6-8). Samples from 15 healthy control volunteers, 12 obese volunteers and 15 type 2 diabetic volunteers were collected. To characterize insulin action *on TP53INP2* expression, the subjects underwent a 3-h euglycemic-hyperinsulinemic (2 mU/kg/min) clamp, as described previously (9). In addition, muscle samples from Bialystok age-matched young lean and overweight subjects were also analyzed. Biopsies from the vastus lateralis muscle were obtained as previously reported (6).

Retrotranscription and competitive-quantitative PCR or real-time PCR was performed from 0.1 μg of total RNA from vastus lateralis muscle samples. Cyclophilin or HPRT mRNA were assayed as controls in real-time PCR assays.

Mouse strains

Transgenic mouse lines (SKM-Tg and SKM-Tg') overexpressing TP53INP2 in skeletal muscle under the control of the Myosin-Light Chain 1 promoter/enhancer were generated (*Mlc1-Tp53inp2*). The open reading frame of *Tp53inp2* was introduced in an EcoRI site in the MDAF2 vector, which contains a 1.5 kb fragment of the *Mlc1* promoter and 0.9 kb fragment of the *Mlc1/3* gene containing a 3' muscle enhancer element (10, 11). The fragment obtained after the digestion of this construct with BssHII was the one used to generate both transgenic mouse lines. Nontransgenic littermates were used as controls for the transgenic animals. Mice were in a C57BL/6J pure genetic background. Four-month-old male mice were used in all experiments, unless indicated.

SKM-KO TP53INP2 mouse line was generated by crossing homozygous *Tp53inp2*$^{loxP/loxP}$ mice with a mouse strain expressing Cre recombinase under the control of the Myosin-Light Chain 1 promoter (12). Non-expressing Cre *Tp53inp2*$^{loxP/loxP}$ littermates were used as controls for knockout animals. Four-month-old male mice were used in all experiments. Mice were in a C57BL/6J pure genetic background.

Mice were kept under a 12-h dark-light period and provided with a standard chow-diet and water *ad libitum*

Food Intake

Animals were placed in individual metabolic cages for 4 days. Mice were acclimated to their new cage environment during the first 48 h. Experimental data were collected over the next 48 h. Food of each mice was weighted every 24h.

Mice treatments

Glucose tolerance tests (GTT) were performed on mice fasted 16 h overnight. Glucose was measured at time 0, followed by intraperitoneal (i.p.) injection of 2g/kg glucose. Blood glucose levels were also measured at 5, 15, 30, 60, 90 and 120 minutes after injection.

Chloroquine was diluted in saline solution and filtered using a 0.22 μm pore diameter filter. Chloroquine solution was injected intraperitoneally twice a day at a dose of 50 mg/kg. SKM-Tg mice were treated for 5 days and SKM-KO mice for 11 days. Saline was injected to control animals.

Streptozotocin was diluted in citrate buffer (pH=4.5) and filtered using a 0.22 μm pore diameter filter. Streptozotocin solution was freshly prepared each time and injected intraperitoneally at a dose of 150 mg/kg on two consecutive days. Control animals were injected with citrate buffer. Four days later animals were sacrificed. Diabetes was confirmed by checking glucose blood levels using an Accu-Check glucose monitor (Roche Diagnostics Corp.). Animals with a glycemia higher than 280 mg/dl were considered diabetic.

For denervation studies mice were anesthetized with 80/10 mg/kg ketamine/xylazine injected intraperitoneally and the sciatic nerve from the right hindlimb was transected. Briefly, the upper part of the right hindlimb was shaved before making and incision to expose the sciatic nerve. A piece of 0.5 cm of the sciatic nerve was removed and,

finally, the incision was closed with surgical stiches. Samples were collected 5 days after denervation.

Protein degradation

Total protein degradation was measured in isolated EDLs (Extensor Digitorum Longus) as described (13, 14). Briefly, muscles were removed and pinned to supports to maintain them at resting length. They were firstly incubated in standard Krebs-Henseleit bicarbonate buffer (5mM glucose) constantly gassed with 95% O_2/5% CO_2 over 30 min at 37º C and under a soft shaking of 45 cycles/min (all the following incubations were performed in these conditions). Secondly, they were transferred to another flask and incubated during 30 min in the same buffer but complemented with 0.5mM cycloheximide (to block tyrosine reuse). Finally, muscles were transferred to another flask and incubated in cycloheximide complemented buffer for 2h. Tyrosine released to the media was measured fluorimetrically as previously described (15)

Proteasome activity in skeletal muscle

Proteasome activity in total homogenates from EDL muscles were measured as reported (16). Briefly, 100 µl of ice-cold PBS with 5mM EDTA was added to 1mg of muscle and sonicated. Tissue lisates were centrifuged at 13.000g for 5 min at 4ºC and supernatants were subjected to protein quantification and diluted until 0.2mg/ml. 50 µl corresponding to 10 µg of total protein were added to 50 µl of the luminescent reagent containing the Ultra-Glo Luciferase and the signal peptides for chymotrypsin-like, trypsin-like and caspase-like acitivities (Promega). To calculate the proteasomal activity, dual measurements with or without specific proteasomal inhibitor adamantane-acetyl-(6-aminohexanoyl)$_3$-(leucinyl)$_3$-vinyl-(methyl)-sulfone

(AdaAhx$_3$L$_3$VS) (Calbiochem) were carried out. After mixing all the components and a 1h preincubation, the resulting luminescence was measured.

In vivo gene transfer

For electrotransfer studies, mTP53INP2-RFP and EGFP-LC3 vectors were purified using a plasmid kit (Endofree; Qiagen, Crawley, UK) and dissolved in 0.9% NaCl. Four month-old mice were anesthetized with ketamine/xylazine and 45 min before electrotransfer muscles were pretreated with hyaluronidase (10 U/muscle) (17, 18). Afterwards, naked plasmids were injected into the tibialis anterior muscle of both hindlimbs. We established that the optimal amount of plasmid to achieve acceptable protein expression was 60 μg DNA for TP53INP2-RFP and EGFP-LC3. Ten pulses of 20 ms each were applied to each hindlimb at 175 V/cm and 1 Hz using an electroporator (ECM 830; BTX, Holliston, MA, USA). Control animals were subjected to the same procedure after injection of an empty vector. Experiments were performed seven days after the electrotransfer.

Fluorescence microscopy in muscle sections

Tibialis anteriors were removed and fixed in PFA 4% (Santa Cruz) rotating for 1 h and 30 min at 4ºC. After being passed through a sucrose gradient from 10% to 30%, muscles were embedded in OCT solution (TissueTek), immediately frozen in liquid nitrogen-cooled isopenthane (Sigma) and stored at -80ºC. 10μm cryosections of tibialis anterior muscle transfected with mTP53INP2-RFP and/or EGFP-LC3 were analyzed using a Leica TCS SP2 AOBS Systems confocal scanning microscope.

EGFP-LC3 positive dots after 16 hours of fasting were counted and normalized for cross-sectional area as described (19).

Histological sample preparation and analysis

For light microscopy, muscles were removed, embedded in OCT solution (TissueTek), immediately frozen in liquid nitrogen-cooled isopenthane (Sigma) and stored at -80ºC. 10 μm cryosections of tibialis anterior or quadriceps muscles were used.

Cryosections were stained with haematoxylin and eosin following standard protocols to check tissue architecture and CSA. CSA was quantified using Image J software.

NADH diaphorase activity staining on cryosections was performed using 0.05M Tris buffer at pH 7.6. Eight mg of NADH and 10 mg of nitro blue tetrazolium were dissolved in 10 mL of Tris buffer and incubated with sections for 30 min at 37ºC.

Succinic dehydrogenase staining on cryosections was performed using 0.2M phosphate buffer at pH 7.6. 270 mg succinic acid and 10 mg nitro blue tetrazolium were freshly dissolved in 10 mL phosphate buffer and incubated with sections for 1h at 37ºC.

TUNEL staining of 10 μm cryosections to detect apoptosis was performed according to the manufacturer's instructions (In Situ Cell Death Detection Kit Fluorescein, Roche).

The Nikon E600 equipped with the Olympus DP 72 camera microscope was used to analyze light and fluorescence cryosection staining. Acquisition software used was Cell F from Olympus.

Immunofluorescence in muscle sections

For immunofluorescence assays, tibialis anterior muscle cryosections were fixed in PFA 4% for 20 minutes at room temperature. After two washes in PBS for 5 minutes, sections were incubated in NH_4Cl (50mM) and glycine (20mM) to reduce the

autofluorescence and permeabilized by incubating them with a solution of 0,1% Triton x-100 in 0,1% sodium citrate during 2 minutes at 4ºC. After two washes in PBS for 5 minutes and blocking during 30 minutes in 10% FBS in PBS, slides were incubated with p62 antibody (Progen) diluted 1/100 in blocking solution during 2 hours. After three, 10 minutes washes in PBS, samples were further incubated in donkey anti-guinea pig Alexa-Fluor 568 conjugated secondary antibodies (Invitrogen) for 1h, followed again by three, 10 minutes washes in PBS. Hoechst33342 (1/2000; Molecular Probes) was used to label DNA. Sections were kept in the dark after secondary antibody incubation. Slides were finally covered using Fluoromount-G (Electron Microscopy Sciences) and let do dry o/n before being stored at 4ºC. Leica TCS SP2 AOBS Systems confocal scanning microscope was used to analyze the immunofluorescence.

Immunohistochemistry in muscle sections

For immunohistochemistry assays, serial tibialis anterior muscle cryosections were obtained and examined by standard immunohistochemical procedures for the expression of myosin heavy chain (MHC) isoforms (20). The primary monoclonal antibodies employed were A4.840 specific for MHCI (Developmental Syudies Hybridoma Bank); A4.74, which stains IIa strongly and IIx weakly (Developmental Studies Hybridoma Bank); and BF-F3 specific for MHCIIb (21).

The Nikon E600 equipped with the Olympus DP 72 camera microscope was used to analyze cryosection staining. Acquisition software used was Cell F from Olympus. Fiber type distribution and CSA were quantified using Image J software.

Electron microscopy

Quadriceps muscles were cut into pieces of about $1mm^3$ and transferred to glass vials filled with 2% parafomaldehyde and 2.5% glutaraldehyde in phosphate buffer. They were kept in the fixative for 24 h at 4ºC. Then, they were washed with the same buffer and post-fixed with 1% osmium tetroxide in the same buffer containing 0.8% potassium ferricyanide at 4ºC. Then the samples were dehydrated in acetone, infiltrated with Epon resin for 2 days, embedded in the same resin orientated for longitudinal sectioning and polymerized at 60ºC during 48 hour. Semithin sections were made in order to corroborate that the orientation was good under the light microscope. When they were found, ultrathin sections were obtained using a Leica Ultracut UC6 ultramicrotome (Leica Microsystems, Vienna, Austria) and mounted on Formvar-coated copper grids. They were stained with 2% uranyl acetate in water and lead citrate. Then, sections were observed under a JEM-1010 electron microscope (Jeol, Japan) equipped with a CCD camera SIS Megaview III and the AnalySIS software.

Micro computed tomography

For *in vivo* scans, mice were anesthetized with 80/10 mg/kg ketamine/xylazine injected intraperitoneally and positioned with the right hindlimb fully extended in the Skyscan 1076 High resolution micro-CT scanner (Kontich, Belgium). The scan set up was the following: source voltage of 50kV; source current of 200 uA; 1mm aluminum filter; rotation step of 0.7 degrees; and frame averaging of 2. Selection of the scan energy and voxel size was based on optimizing the requirements of scanning time and tissue details in a way that minimized mice exposure to radiation. The right hindlimb was scanned at an isotropic voxel size of 35 μm and with 360º of scan rotation.

Scans were reconstructed using the N*Recon* software provided by *Skyscan*. Reconstruction parameters were the following: smoothing of 4; ring artifact correction of 5; beam hardening correction of 30%; minimum for CS to image conversion of 0.00; and maximum for CS to image conversion of 0.04.

For image analysis and calculations the *CTscan Skyscan* software was applied. The region selected for the analysis was the part of the right back leg found along the entire fibula. By doing so, we always considered the same region from all mice. The lean tissue volume from that region was obtained.

Muscle regeneration studies

Animals were anesthetized with 80/10 mg/kg ketamine/xylazine injected intraperitoneally. Regeneration of skeletal muscle was induced by intramuscular injection of 75 μL of 1 μM Cardiotoxin (Latoxan) in the tibialis anterior muscle of the mice (22). Seven days post-injury, muscles were removed and CSA analyzed as described.

Cell culture

C2C12 myoblasts were grown in monolayer culture in Dulbecco's modified Eagle's medium (DMEM) containing 10% (v/v) fetal bovine serum (FBS), 25mM Hepes and 1% (v/v) antibiotics (10,000 units/mL penicillin G and 10 mg/mL streptomycin). 80% confluent myoblasts were differentiated by using a differentiation medium consisting in DMEM supplemented with 2% horse serum and 1% (v/v) antibiotics (10,000 units/mL penicillin G and 10 mg/mL streptomycin)

At day 3 of differentiation, myotubes were transduced for 30 h at a multiplicity of infection (moi) of 50 pfu/cell and all the experiments were performed at day 5 of differentiation. LacZ coding adenoviruses were used as control.

Adenoviruses were generated by transfection of the adenoviral expression vectors (Virapower System, Invitrogen) in human embryonic kidney cell line (HEK 293A). The adenoviruses generated were then amplified in HEK 293A cells, titrated using the Adeno-XTM Rapid Titer kit (Clontech) and used directly for cell transduction.

C2C12 cells were treated with bafilomycin A1 (200nM) for three hours or with puromycin (50 μg/mL) for four hours when indicated.

HEK293T cells were grown in DMEM containing 10% FBS, 1% Penicillin/Streptomycin and HEPES. Starvation, when indicated, was induced by 2 h incubation in HBSS media supplemented with 1% Penicillin/Streptomycin.

Immunofluorescence in C2C12 myotubes

C2C12 were fixed in PFA 4% for 10 minutes at room temperature. After two washes in PBS for 10 minutes, cells were incubated in NH_4Cl (50mM) and glycine (20mM) to reduce the autofluorescence and permeabilized with a solution of 0,1% Triton x-100 in PBS during 10 minutes at room temperature. After two washes in PBS for 10 minutes and blocking during 30 minutes in 10% FBS in PBS, slides were incubated with the corresponding primary antibodies diluted in blocking solution during 1 hour. After three, 10 minutes washes in PBS, samples were further incubated with the corresponding secondary antibodies for 1h, followed again by three, 10 minutes washes in PBS. Hoechst33342 (1/2000; Molecular Probes) was used to label DNA. Finally, cells were covered using Fluoromount-G (Electron Microscopy Sciences) and

let to dry o/n before being stored at 4ºC. Leica TCS SP2 AOBS Systems confocal scanning microscope was used to analyze the immunofluorescence.

The following primary antibodies were used: p62 (1/100 Progen), LC3 raised in rabbit (1/200 MBL), LC3 raised in mouse (1/25 MBL), Ub (FK2) (1/500 ENZO life sciences), TP53INP2 (1/150 generated in our laboratory).

The following secondary antibodies were used: goat anti-guinea pig conjugated with Alexa-Fluor 568, goat anti-mouse conjugated with Alexa-Fluor 568, donkey anti-mouse conjugated with Alexa-Fluor 647, goat anti-rabbit conjugated with Alexa-Fluor 488 (1/250 Invitrogen for all the antibodies).

Protein extraction and Western Blotting

Skeletal muscle homogenates for Western Blot analyses were obtained by powdering 30 mg of frozen muscle and incubating them in lysis buffer (50 mM Tris pH 6.8, 10% (v/v) glycerol, 2% SDS and protease inhibitors cocktail tablet, Roche) during 5 minutes at 95ºC with 800 rpm shaking. After that, homogenates were centrifugated at 700 g for 10 min and 4ºC to remove cell debris.

Homogenates for Western Blot analyses from cell cultures were obtained by collecting the cells in ice-cold PBS 1X, homogenizing them with a douncer in lysis buffer (50 mM Tris pH 7.5, 150 mM NaCl, 1% Triton X-100, 1 mM EDTA, 1 mM sodium ortovanadate, 50 mM NaF, 5 mM sodium pyrophosphate and protease inhibitors cocktail tablet, Roche) and centrifugating them at 700 g for 10 min and 4ºC to remove nuclei, cell debris and floating cells.

Proteins from total homogenates were resolved in 7.5%, 10%, 12.5% or 15% acrylamide gels for SDS-PAGE and transferred to Immobilon membranes (Millipore).

The following antibodies were used: p62 (1/1000 Progen), NBR1 (1/500 Abcam), Ub (FK2) (1/6000 ENZO life sciences), LC3 (1/1000 MBL), Porin (1/5000 Calbiochem), α-Tubulin (1/8000 Sigma), TP53INP2 (1/500 generated in our laboratory) (23), GFP (1/3000 Abcam), HA (1/1000 Roche). Proteins were detected by the ECL method as described (24) and quantified by scanning densitometry.

Gene expression analysis

RNA from tissues was extracted using a protocol combining TRIzol reagent (Invitrogen) and RNAeasy® minikit columns (Qiagen) following the manufacturer's instructions. RNA was reverse-transcribed with the SuperScript RTIII kit (Invitrogen). Quantitative real-time PCR was performed using the ABI Prism 7900 HT real-time PCR machine (Applied Biosystems) and the SYBR® Green PCR Master Mix or the Taqman Probes 20X (Applied Biosystems). All measurements were normalized to *Beta-actin* and *Gapdh*.

The following Sybr Green primers were used: *Beta-actin*, Fwd: GGTCATCACTATTGGCAACGA, Rev: GTCAGCAATGCCTGG; *Gapdh*: Fwd: CATGGCCTTCCGTGTTCCTA, Rev: GCGGCACGTCAGATCCA; *Tp53inp2*, Fwd: AACCACAGCCTGCTTCTAATACCTT, Rev: TCAGCCAGTCTCAACACAAAAC AC; *LC3b*, Fwd: AGCTCTTTGTTGGTGTGTAACTGTCT, Rev: TTGTCCTCACA GCTGACATGTATG; *p62*, Fwd: CCCAGTGTCTTGGCATTCTT, Rev: AGGGAAA GCAGAGGAAGCTC; *Nbr1*, Fwd: CCCCAGATTGGTTTACAAGC, Rev: TCCAC CGTTTCCTTAACCAC.

Transcriptomic analysis

Microarray services were provided by the IRB Functional Genomics Core Facility, including quality control tests of total RNA using Agilent Bioanalyzer and Nanodrop spectrophotometry. Briefly, cDNA library preparation and amplification were performed from 25 ng total RNA using WTA2 (Sigma-Aldrich) with 17 cycles of amplification. 8µg cDNA were subsequently fragmented by DNaseI and biotinylated by terminal transferase obtained from GeneChip Mapping 250K Nsp Assay Kit (Affymetrix). Hybridization mixture was prepared according to Affymetrix protocol. Each sample was hybridized to a Mouse Genome 430 PM strip (Affymetrix). Arrays were washed and stained in a Fluidics Station 450 (Fluidics protocol FS450_002) and scanned in a GeneChip Scanner 3000 (both Affymetrix) according to manufacturer's recommendations. CEL files were generated from DAT files using GCOS software (Affymetrix).

All microarray analyses were perfomed using Bioconductor (25). Background correction, quantile normalization and median polish summarization was performed as implemented in bioconductor's affy package (26). Some groups of mice had the same parents. A semi-parametric empirical Bayes procedure based on moderated t-tests as implemented in limma package was performed to select the enriched genes setting the Bayesian FDR at 10% (27). Additionally, only genes with an absolute fold change value bigger than 1.3 were considered differentially expressed.

Immunoprecipitation assays

For normal immunoprecipitation assays, HEK 293T cells were plated onto 6 cm plates and transfected with corresponding plasmids. 24 h after transfections, cell were lysed in Flag lysis buffer (50 mM Tris pH 7.4, 150 mM NaCl, 1% Triton X-100, 1 mM EDTA, 10 mM NEM and protease and phosphatase inhibitors cocktail tablets,

Roche), in another lysis buffer for GFP-Trap pull down (10 mM Tris pH 7.5, 150 mM NaCl, 0.5% NP-40, 0.5 mM EDTA, 10 mM NEM and protease and phosphatase inhibitors cocktail tablets, Roche) or in RIPA buffer for HA pull down. Proteins were immunoprecipitated with Flag, HA or GFP resins according to manufacturers instructions.

For semi-direct immunoprecipitation assays, 40 μg of His-monoUb, 20 μg of His-UbK48 or 20 μg of His-UbK63 were coupled to cobalt resin. After 2 h of incubation at 4 ºC, resin was washed twice with PBS and Flag-TP53INP2 previously pulled down with Flag resin was added to the cobalt beads. After 2 h of incubation, beads were washed with washing buffer (50mM Imidazol, 500mM NaCla, 1nM Na_3VO_4 in milliQ water) eluted with elution buffer (250mM Imidazol, 300mM NaCla in milliQ water).

Supplemental references

1. Mauvezin, C., Sancho, A., Ivanova, S., Palacin, M., and Zorzano, A. 2012. DOR undergoes nucleo-cytoplasmic shuttling, which involves passage through the nucleolus. *FEBS Lett*.

2. Tasdemir, E., Maiuri, M.C., Tajeddine, N., Vitale, I., Criollo, A., Vicencio, J.M., Hickman, J.A., Geneste, O., and Kroemer, G. 2007. Cell cycle-dependent induction of autophagy, mitophagy and reticulophagy. *Cell Cycle* 6:2263-2267.

3. Sancho, A., Duran, J., Garcia-Espana, A., Mauvezin, C., Alemu, E.A., Lamark, T., Macias, M.J., DeSalle, R., Royo, M., Sala, D., et al. 2012. DOR/Tp53inp2 and Tp53inp1 constitute a metazoan gene family encoding dual regulators of autophagy and transcription. *PLoS One* 7:e34034.

4. Dantuma, N.P., Groothuis, T.A., Salomons, F.A., and Neefjes, J. 2006. A dynamic ubiquitin equilibrium couples proteasomal activity to chromatin remodeling. *J Cell Biol* 173:19-26.

5. Kamitani, T., Kito, K., Nguyen, H.P., and Yeh, E.T. 1997. Characterization of NEDD8, a developmentally down-regulated ubiquitin-like protein. *J Biol Chem* 272:28557-28562.

6. Andreelli, F., Laville, M., Ducluzeau, P.H., Vega, N., Vallier, P., Khalfallah, Y., Riou, J.P., and Vidal, H. 1999. Defective regulation of phosphatidylinositol-3-kinase gene expression in skeletal muscle and adipose tissue of non-insulin-dependent diabetes mellitus patients. *Diabetologia* 42:358-364.

7. Ducluzeau, P.H., Perretti, N., Laville, M., Andreelli, F., Vega, N., Riou, J.P., and Vidal, H. 2001. Regulation by insulin of gene expression in human

skeletal muscle and adipose tissue. Evidence for specific defects in type 2 diabetes. *Diabetes* 50:1134-1142.

8. Debard, C., Laville, M., Berbe, V., Loizon, E., Guillet, C., Morio-Liondore, B., Boirie, Y., and Vidal, H. 2004. Expression of key genes of fatty acid oxidation, including adiponectin receptors, in skeletal muscle of Type 2 diabetic patients. *Diabetologia* 47:917-925.

9. Laville, M., Auboeuf, D., Khalfallah, Y., Vega, N., Riou, J.P., and Vidal, H. 1996. Acute regulation by insulin of phosphatidylinositol-3-kinase, Rad, Glut 4, and lipoprotein lipase mRNA levels in human muscle. *J Clin Invest* 98:43-49.

10. Rosenthal, N., Kornhauser, J.M., Donoghue, M., Rosen, K.M., and Merlie, J.P. 1989. Myosin light chain enhancer activates muscle-specific, developmentally regulated gene expression in transgenic mice. *Proc Natl Acad Sci U S A* 86:7780-7784.

11. Otaegui, P.J., Ferre, T., Riu, E., and Bosch, F. 2003. Prevention of obesity and insulin resistance by glucokinase expression in skeletal muscle of transgenic mice. *FASEB J* 17:2097-2099.

12. Bothe, G.W., Haspel, J.A., Smith, C.L., Wiener, H.H., and Burden, S.J. 2000. Selective expression of Cre recombinase in skeletal muscle fibers. *Genesis* 26:165-166.

13. Wang, X., Hu, Z., Hu, J., Du, J., and Mitch, W.E. 2006. Insulin resistance accelerates muscle protein degradation: Activation of the ubiquitin-proteasome pathway by defects in muscle cell signaling. *Endocrinology* 147:4160-4168.

14. Tawa, N.E., Jr., Kettelhut, I.C., and Goldberg, A.L. 1992. Dietary protein deficiency reduces lysosomal and nonlysosomal ATP-dependent proteolysis in muscle. *Am J Physiol* 263:E326-334.

15. Waalkes, T.P., and Udenfriend, S. 1957. A fluorometric method for the estimation of tyrosine in plasma and tissues. *J Lab Clin Med* 50:733-736.

16. Strucksberg, K.H., Tangavelou, K., Schroder, R., and Clemen, C.S. 2010. Proteasomal activity in skeletal muscle: a matter of assay design, muscle type, and age. *Anal Biochem* 399:225-229.

17. Franckhauser, S., Elias, I., Rotter Sopasakis, V., Ferre, T., Nagaev, I., Andersson, C.X., Agudo, J., Ruberte, J., Bosch, F., and Smith, U. 2008. Overexpression of Il6 leads to hyperinsulinaemia, liver inflammation and reduced body weight in mice. *Diabetologia* 51:1306-1316.

18. Long, F., Zhang, X.M., Karp, S., Yang, Y., and McMahon, A.P. 2001. Genetic manipulation of hedgehog signaling in the endochondral skeleton reveals a direct role in the regulation of chondrocyte proliferation. *Development* 128:5099-5108.

19. Mizushima, N., Yamamoto, A., Matsui, M., Yoshimori, T., and Ohsumi, Y. 2004. In vivo analysis of autophagy in response to nutrient starvation using transgenic mice expressing a fluorescent autophagosome marker. *Mol Biol Cell* 15:1101-1111.

20. Serrano, A.L., Murgia, M., Pallafacchina, G., Calabria, E., Coniglio, P., Lomo, T., and Schiaffino, S. 2001. Calcineurin controls nerve activity-dependent specification of slow skeletal muscle fibers but not muscle growth. *Proc Natl Acad Sci U S A* 98:13108-13113.

21. Schiaffino, S., Gorza, L., Sartore, S., Saggin, L., Ausoni, S., Vianello, M., Gundersen, K., and Lomo, T. 1989. Three myosin heavy chain isoforms in type 2 skeletal muscle fibres. *J Muscle Res Cell Motil* 10:197-205.

22. Kherif, S., Lafuma, C., Dehaupas, M., Lachkar, S., Fournier, J.G., Verdiere-Sahuque, M., Fardeau, M., and Alameddine, H.S. 1999. Expression of matrix metalloproteinases 2 and 9 in regenerating skeletal muscle: a study in experimentally injured and mdx muscles. *Dev Biol* 205:158-170.

23. Baumgartner, B.G., Orpinell, M., Duran, J., Ribas, V., Burghardt, H.E., Bach, D., Villar, A.V., Paz, J.C., Gonzalez, M., Camps, M., et al. 2007. Identification of a novel modulator of thyroid hormone receptor-mediated action. *PLoS One* 2:e1183.

24. Enrique-Tarancon, G., Castan, I., Morin, N., Marti, L., Abella, A., Camps, M., Casamitjana, R., Palacin, M., Testar, X., Degerman, E., et al. 2000. Substrates of semicarbazide-sensitive amine oxidase co-operate with vanadate to stimulate tyrosine phosphorylation of insulin-receptor-substrate proteins, phosphoinositide 3-kinase activity and GLUT4 translocation in adipose cells. *Biochem J* 350 Pt 1:171-180.

25. Gentleman, R.C., Carey, V.J., Bates, D.M., Bolstad, B., Dettling, M., Dudoit, S., Ellis, B., Gautier, L., Ge, Y., Gentry, J., et al. 2004. Bioconductor: open software development for computational biology and bioinformatics. *Genome Biol* 5:R80.

26. Irizarry, R.A., Hobbs, B., Collin, F., Beazer-Barclay, Y.D., Antonellis, K.J., Scherf, U., and Speed, T.P. 2003. Exploration, normalization, and summaries of high density oligonucleotide array probe level data. *Biostatistics* 4:249-264.

27. Rossell, D., Guerra, R., and Scott, C. 2008. Semi-parametric differential expression analysis via partial mixture estimation. *Stat Appl Genet Mol Biol* 7:Article15.

Supplementary Table 1. List of regulated genes in skeletal muscle from SKM-Tg mice

probeset	entrez	symbol	genename	Tg.mean	Wt.mean	foldChange	probDE	rej
1452318_a_a	15511	Hspa1b	heat shock prote	6.45100472	7.42502876	-1.9643119	0.99257576	-1
1417793_at	54396	Irgm2	immunity-relate	5.48580358	6.03895392	-1.4672862	0.98268075	-1
1444222_x_a	NA	NA	NA	8.03970559	8.57080507	-1.44503	0.97128002	-1
1449109_at	216233	Socs2	suppressor of cy	5.35671201	6.23470065	-1.8378113	0.96996502	-1
1427233_at	110796	Tshz1	teashirt zinc fing	5.92352092	6.37182254	-1.3644331	0.96274058	-1
1449357_at	66952	2310030G06	RIKEN cDNA 231	4.85435023	5.60226615	-1.6793651	0.96200657	-1
1450044_at	14369	Fzd7	frizzled homolog	6.49159357	7.17891259	-1.6102883	0.95702803	-1
1426519_at	18451	P4ha1	procollagen-prol	7.11544697	7.50403187	-1.3091087	0.94980921	-1
1454877_at	214791	Sertad4	SERTA domain c	4.40546725	4.82328209	-1.3359026	0.94511543	-1
1438511_a_a	66214	1190002H23	RIKEN cDNA 119	9.23325793	9.67137292	-1.354833	0.94253329	-1
1427344_s_a	75141	Rasd2	RASD family, me	5.70128748	7.02905718	-2.5101432	0.93540899	-1
1433983_at	215748	Cnksr3	Cnksr family mer	6.50432748	7.11251649	-1.5243445	0.93469721	-1
1439389_s_a	50918	Myadm	myeloid-associat	7.46260117	8.1447866	-1.6045685	0.9336047	-1
1455903_at	210789	Tbc1d4	TBC1 domain far	8.10612864	8.53055734	-1.342041	0.93357094	-1
1439859_at	319801	9630033F20F	RIKEN cDNA 963	8.69436291	9.26951868	-1.4898383	0.93292534	-1
1424473_at	245841	Polr2h	polymerase (RNA	6.33489068	6.80084228	-1.3812281	0.93229356	-1
1427329_a_a	16019	Ighm	immunoglobulin	7.24395783	8.79036432	-2.9208869	0.93074416	-1
1433776_at	108927	Lhfp	lipoma HMGIC fu	6.24811473	6.66610578	-1.3360658	0.9293776	-1
1428736_at	107022	Gramd3	GRAM domain c	6.85666546	7.40417635	-1.4615619	0.92780231	-1
1451833_a_a	84505	Setdb1	SET domain, bifu	5.41406075	5.80699496	-1.3130612	0.92403782	-1
1452218_at	104479	Ccdc117	coiled-coil doma	5.6918141	6.27529767	-1.4984631	0.92045887	-1
1452707_at	70788	Klhl30	kelch-like 30 (Dr	9.75042843	10.3917669	-1.5597756	0.91732193	-1
1419389_at	23984	Pde10a	phosphodiestera	6.44869346	7.1753994	-1.6548563	0.91055081	-1
1448299_at	20510	Slc1a1	solute carrier far	4.95869293	5.48493143	-1.4401694	0.9030236	-1
1417136_s_a	20817	Srpk2	serine/arginine-r	7.75544277	8.14680461	-1.3116309	0.8978068	-1
1417312_at	50781	Dkk3	dickkopf homolc	5.82124045	6.59271793	-1.7070171	0.89739189	-1

1423170_at	24074	Taf7	TAF7 RNA polym	6.65773126	7.2929455	-1.5531684	0.89456054	-1
1431281_at	68701	Ppp1r27	protein phospha	8.3669739	9.62025841	-2.3838352	0.8937858	-1
1449945_at	170826	Ppargc1b	peroxisome prol	7.02659364	7.59656025	-1.4844892	0.88559456	-1
1418003_at	66214	1190002H23I	RIKEN cDNA 119	8.46828292	8.89651165	-1.3455805	0.87983886	-1
1454637_at	246293	Klhl8	kelch-like 8 (Dro	7.15851173	7.6267262	-1.3833963	0.87052087	-1
1433454_at	99382	Abtb2	ankyrin repeat a	4.63204988	5.05139532	-1.3373207	0.86873139	-1
1421811_at	21825	Thbs1	thrombospondir	6.84238434	7.33067225	-1.4027792	0.86575979	-1
1456271_at	381126	Fam59a	family with sequ	6.34301036	7.04021455	-1.6213597	0.86552105	-1
1422506_a_a	13014	Cstb	cystatin B	8.27081587	8.6678639	-1.3168108	0.86417209	-1
1437273_at	330723	Htra4	HtrA serine pept	3.79763418	4.4834376	-1.6085975	0.86058224	-1
1437224_at	68585	Rtn4	reticulon 4	7.08862597	7.65829604	-1.4841841	0.85458159	-1
1437348_at	67948	Fbxo28	F-box protein 28	5.63611106	6.11444161	-1.3931306	0.85394802	-1
1430984_at	54375	Azin1	antizyme inhibit	4.66242925	5.09653973	-1.3510776	0.8501644	-1
1456405_at	23856	Dido1	death inducer-ol	5.46600014	6.05243811	-1.5015349	0.8468354	-1
1426432_a_a	54403	Slc4a4	solute carrier far	7.28601297	7.75477624	-1.3839226	0.84240644	-1
1422567_at	63913	Fam129a	family with sequ	6.04511272	6.43909004	-1.314011	0.84032199	-1
1426179_a_a	65960	Twsg1	twisted gastrulat	7.33653681	7.73795177	-1.3208027	0.83961101	-1
1456642_x_a	20194	S100a10	S100 calcium bir	8.25922982	8.72352659	-1.3796447	0.8359326	-1
1443475_at NA		NA	NA	5.99512202	5.40644228	1.50386987	0.98051586	1
1423835_at	218820	Zfp503	zinc finger prote	6.00505914	5.50483904	1.41442934	0.96175298	1
1449804_at	18948	Pnmt	phenylethanolar	7.98607344	6.80292359	2.27072005	0.93758847	1
1449351_s_a	54635	Pdgfc	platelet-derived	4.09238919	3.70603872	1.30708274	0.93165865	1
1447623_s_a	18760	Prkd1	protein kinase D	6.88081762	6.47755628	1.32249415	0.92013159	1
1458635_at	403183	4832428D23I	RIKEN cDNA 483	4.79521075	4.12096488	1.59576241	0.90361596	1
1445186_at	20856	Stc2	stanniocalcin 2	6.0500573	5.54823965	1.41599645	0.89822509	1
1425382_a_a	11829	Aqp4	aquaporin 4	6.45455068	6.05045719	1.32325719	0.89605357	1
1443062_at	319974	Auts2	autism susceptib	3.76430859	3.29770193	1.3818554	0.88492872	1
1440388_at NA		NA	NA	5.64632849	5.25816632	1.30872517	0.87863292	1
1455007_s_a	108682	Gpt2	glutamic pyruvat	9.42380068	8.87002117	1.46792627	0.8629621	1

1460269_at	18948	Pnmt	phenylethanolar	7.51499647	5.97278855	2.9123988	0.86265393	1
1448636_at	59011	Myoz1	myozenin 1	10.1495642	9.73299686	1.33474794	0.85796653	1

Supplementary Table 2. List of regulated genes in skeletal muscle from SKM-KO mice

probeset	entrez	symbol	genename	KO.mean	LoxP.mean	foldChange	probDE	rej
1452646_at	68728	Trp53inp2	transforma	8.648208268	10.994374	-5,08471084985868	0.9999905579	-1
1429569_a_at	76380	Ccdc46	coiled-coil (	4.193501101	4.5791885	-1.306482138	0.9816705285	-1
1427011_a_at	14768	Lancl1	LanC (bacte	7.944221083	8.3942453	-1.366063234	0.9531632289	-1
1426166_at	17844	Mup5	major urina	3.794131227	4.1769652	-1.303900706	0.9396253762	-1
1441413_at	NA	NA	NA	6.35599078	6.8111729	-1.370955875	0.9192500608	-1
1454559_at	50795	Sh3bgr	SH3-bindin	6.815474899	7.3189839	-1.417657428	0.8815602721	-1
1437358_at	69368	Wdfy1	WD repeat	6.908000434	5.5527303	2.558450237	0.9999752745	1
1424749_at	69368	Wdfy1	WD repeat	6.921956822	5.6088632	2.484737724	0.9999065021	1
1425942_a_at	14758	Gpm6b	glycoprotei	6.326457446	5.8125932	1.427869638	0.9974715977	1
1450014_at	12737	Cldn1	claudin 1	6.770022753	6.1566008	1.529883659	0.9930649384	1
1423153_x_at	12628	Cfh	complemer	3.934848209	3.4620363	1.387811727	0.9853189770	1
1422847_a_at	18753	Prkcd	protein kin	5.926399321	5.4301376	1.410553842	0.9778631584	1
1436914_at	329506	Ctdspl2	CTD (carbo	4.837440985	4.4247089	1.331204335	0.9771727139	1
1434333_a_at	101540	Prkd2	protein kin	4.363108044	3.9536061	1.328227241	0.9760571900	1
1437932_a_at	12737	Cldn1	claudin 1	4.689096994	4.1071515	1.49686646	0.9613511266	1
1443814_x_at	13036	Ctsh	cathepsin H	5.201876173	4.7244581	1.392249756	0.9565603966	1
1435126_at	252864	Dusp15	dual specifi	4.89957816	4.5182813	1.30251218	0.9559297758	1
1450606_at	18948	Pnmt	phenyletha	5.693040699	5.2988402	1.314214215	0.9498744182	1
1440084_at	NA	NA	NA	7.545953922	7.0890702	1.372573775	0.9488066865	1
1450876_at	12628	Cfh	complemer	4.217238345	3.7966389	1.338483558	0.9429250867	1
1455978_a_at	17181	Matn2	matrilin 2	5.427051059	4.8240835	1.518837497	0.9424721638	1
1435588_at	69368	Wdfy1	WD repeat	4.332164802	3.5081696	1.770301615	0.9284612835	1
1445621_at	NA	NA	NA	5.253443232	4.8434764	1.328655289	0.9254114694	1
1459930_at	NA	NA	NA	4.613975299	4.0678866	1.460121814	0.9166188512	1
1434458_at	14313	Fst	follistatin	4.142154685	3.7139869	1.34552371	0.8939522343	1
1458635_at	403183	4832428D23Ril	RIKEN cDN/	4.673686349	4.1829415	1.405170168	0.8832599740	1
1420666_at	13447	Doc2b	double C2,	4.322280715	3.6687223	1.573043318	0.8770096239	1
1421321_a_at	56349	Net1	neuroepith	8.611904159	8.1963249	1.33383408	0.8761245495	1
1437747_at	140630	Ube4a	ubiquitinati	9.041124008	8.6563085	1.305692827	0.8692063601	1
1444396_at	68728	Trp53inp2	transforma	6.069891492	5.5766721	1.407582366	0.8646301245	1
1415911_at	16210	Impact	imprinted a	5.568065196	5.1057745	1.377727584	0.8599209615	1

1433174_a_at	71384	5430440L12Rik	RIKEN cDNA	5.661233757	5.2747023	1.307246699	0.8593673220 1

Supplementary table 3. Characteristics of the obese and type 2 diabetic subjects (Lyon study)

	Lean control	Obese	Type 2 Diabetes
Men / Women	6/7	6/9	8/10
Age (years)	51 ± 4	44 ± 5	52 ± 2
BMI (kg/m^2)	22.3 ± 0.6	35.0 ± 2.4 *	30.8 ± 0.9 *
Glucose (mmol/l)	4.8 ± 0.1	5.0 ± 0.2	12.1 ± 0.7 *
Insulin (pmol/l)	34 ± 2	64 ± 6 *	57 ± 3 *
Glucose disposal rate (during the clamp) ($mg.kg^{-1}.min^{-1}$)	9.9 ± 1.1	4.9 ± 0.8*	3.6 ± 0.4 *

Data are means ± SEM. * indicates statistically significant differences compared to the control group, at $p<0.05$.

Supplementary table 4. Characteristics of the healthy subjects subjected to 3h of euglycemic-hyperinsulinemic clamp (Lyon study)

Men / Women	4/7
Age	24 ± 1
BMI	22 ± 0.6
Glucose (mmol/l)	4.4 ± 0.1
Insulin (pmol/l)	25 ± 6
Glucose disposal rate (during the clamp) ($mg.kg^{-1}.min^{-1}$)	10.1 ± 0.8

Data are means ± SEM.

Supplementary table 5. Characteristics of the obese nondiabetic subjects subjected to 3h of euglycemic-hyperinsulinemic clamp (Lyon study)

Men / Women	1/5
Age	44 ± 8
BMI	35 ± 2
Glucose (mmol/l)	5.0 ± 0.2
Insulin (pmol/l)	57 ± 3
Glucose disposal rate (during the clamp) ($mg.kg^{-1}.min^{-1}$)	5.2 ± 0.8

Data are means ± SEM.

Supplementary table 6. Characteristics of the type 2 diabetic subjects subjected to 3h of euglycemic-hyperinsulinemic clamp (Lyon study)

Men / Women	8/10
Age	52 ± 2
BMI	30.8 ± 0.9
Glucose (mmol/l)	12.1 ± 0.7
Insulin (pmol/l)	57 ± 3
Glucose disposal rate (during the clamp) ($mg.kg^{-1}.min^{-1}$)	3.6 ± 0.4

Data are means ± SEM.

Supplementary table 7. Characteristics of the overweight men (Bialystok study)

	Lean control	Overweight
Age (years)	23 ± 2	23 ± 2
BMI (kg/m^2)	22.2 ± 1.8	27.1 ± 1.6 *
Glucose (mmol/l)	4.9 ± 0.6	5.3 ± 1.1
Insulin (□U/ml)	9.4 ± 4.6	9.0 ± 2.3
Glucose disposal rate (during the clamp) ($mg.kg^{-1}.min^{-1}$)	9.2 ± 2.6	6.9 ± 2.2*

Data are Means ± SEM. * indicates statistically significant differences compared to the control group, at $p<0.05$.

Supplementary table 8. Characteristics of the healthy subjects shown in Figure 7E (Bialystok study)

Men / Women	79/11
Age	23 ± 2
BMI	25.0 ± 2.3
Glucose (mmol/l)	4.7 ± 0.4
Insulin (mU/ml)	10.6 ± 4.9

Data are Means ± SEM.